4-2007

Experimental Measurements and Mathematical Modeling of the Rigid Capillary Dewatering

Vrajesh N. Chokshi

EXPERIMENTAL MEASUREMENTS AND MATHEMATICAL MODELING OF THE RIGID CAPILLARY DEWATERING

by

Vrajesh N. Chokshi

A Thesis
Submitted to the
Faculty of The Graduate College
in partial fulfillment of the
requirements for the
Degree of Master of Science in Engineering (Mechanical)
Department of Mechanical and Aeronautical Engineering

Western Michigan University
Kalamazoo, Michigan
April 2007

ACKNOWLEDGMENTS

I want to express my warm appreciation to Dr. Peter and Dr. Liou for giving me this opportunity, support, and guidance. I would not have pursued the graduate work and avalanche of the thesis experience without their professional guidance. I appreciate them; and also to Dr. Merati, for discussing with me some of the difficult points in the thesis work.

I would like to acknowledge *Procter & Gamble* for providing RCD technology and financial support to this thesis work. I would like to thank Asten Johnson inc. for providing fabric. I am grateful to Reak Reams, Jim Singleton, Kim Ketchum, Robert Rielly, Mathew Stoops and other WMU pilot plant workers for their hard work and technical support to mount Rigid Capillary Dewatering Technology and run the machine with desired parameters.

Finally, I would like to thank my mother, Hemlataben Chokshi and sister, Purvi Shah, who provided moral backing to continue my education. Their constant support allowed me to focus on my education and to get the most of the opportunities provided throughout my graduate studies.

Vrajesh N. Chokshi

EXPERIMENTAL MEASUREMENTS AND MATHEMATICAL MODELING OF THE RIGID CAPILLARY DEWATERING

Vrajesh N. Chokshi, M.S.E.

Western Michigan University, 2007

Rigid Capillary Dewatering (RCD) technology is a process in which water is removed from a wet paper web by capillary dewatering action without excessive mechanical compaction of the fiber furnish. Operating conditions on the Rigid Capillary Pressing (RCP) roll, and properties of paper and pulp determines the dewatering behavior of the RCD technology.

The dewatering behavior of the RCD technology is studied in four sets of experiments performed using different operating conditions, on a paper pilot machine at a Western Michigan University (WMU) facility. The solids content of the paper web before and after the RCP roll in the press section for basis weight ranging from 35lb/3000ft^2 to 70 lb/3000ft^2, press load ranging from 15 pli to 60 pli. For the operating conditions given above, the change in the solids content can be obtained in the range of -2 to 15%. Moreover, a mathematical model to understand the dewatering behavior of paper web in initial stage of dewatering was derived and solved.

TABLE OF CONTENTS

Table of Contents—continued

Table of Contents—continued

LIST OF TABLES

LIST OF FIGURES

List of Figures—continued

NOMENCLATURE

F_c	Force out of cylinder
F_{ceff}	Effective force on the roller
L_{proll}	Length of pivoting point to the cylinder load point
L_{fabric}	Width of the fabric
W_{roller}	Weight of press roll
W_{paper}	Width of paper web
t	Time
h	Penetration depth
B	Capillary width
W	Capillary length
μ	Viscosity of fluid
P	Density of fluid
g	Gravitational constant
ϕ_d	Angle between capillary wall and tangent to surface front
σ	Surface tension
ω	Angular velocity
Δp	Pressure difference across limiting orifice medium
r_0	Radius of capillary
l	Height of the sink fluid
R	Radius of rotation and radius of the RCP cylinder
L	Length of the first layer of Capillary medium
v	Velocity of fluid front

Nomenclature—continued

R_e	Reynolds number
$r, , z$	Cylindrical coordinate parameters
v_θ	Rotational velocity of fluid
v_r	Radial velocity of fluid
v_z	Velocity of fluid in Z-direction
ΣF_z	Summation of Forces acting in Z-direction
M_b	First term on the right side of equation (4.2)
M_s	Second term on the right side of equation (4.2)
F_b	Body forces acting on the control volume
F_s	Surface forces acting on the control volume
F_{bg}	Gravitational force on the control volume
F_{bc}	Centrifugal force on control volume
F_{sc}	Surface forces acting on cylindrical surface
F_{sf}	Surface forces acting on surface front
F_{sfc}	Centrifugal force of sink fluid
F_{sft}	Force due to surface tension
F_{sfp}	Pressure force on surface front
F_{sfg}	Gravitational force of sink fluid
τ_w	Shear stress on capillary wall

CHAPTER I

INTRODUCTION

The pulp and paper industry in United States employed more than 170,000 workers with an annual payroll of approximately $55 billion in year 2001. Annual industry shipments are worth more than $50 billion according to annual survey of manufacturers (ASM) in year 2001.

But paper, what is it? Paper is a thin, flat material produced by the compression and dewatering of wood pulp. It is also a material used for writing, printing, drawing, wrapping packages, and covering walls. Paper is made in thin sheets from wood pulp, rags or, straw[1]. Try to imagine a single day of your life spent without a single item of paper. Everyone uses paper on daily basis. This includes the newspaper you read in the morning, the paper towel used to clean coffee spilled at breakfast, all the files and papers on your work desk, and maybe my thesis that is in your hand right now!

Paper manufacturing

Paper was invented according to the Chinese history in 105 A.D. by the minister Ts'ai L Lun[2]. However, today's paper manufacturing process is not an easy task. Before the pulp comes to the papermaking machine, it goes through a chipping process. The process begins by cutting down trees and stripping the bark. The stripped logs are then cut into pieces and ground into the wood chips. The wood chips must be separated further to be suitable for sheet forming. There are two main processes to accomplish this: mechanically by grinding the wood chips or by chemically cooking the chips. If the wood

chips are mechanically prepared, they are further ground using a wood chip refiner. When the wood chips are cooked and treated chemically, lignin, a substance that acts as glue in native wood, is dissolved from the fiber material. When lignin is dissolved, the wood fibers no longer hold together and remain suspended in water. By means of dilution with large quantities of water, fiber aggregation is prevented. This completes the pulping process[3].

After the pulp is prepared, it is ready for the paper machine. The purpose of the paper machine is to form thin paper sheet and remove water from the pulp. A pictorial diagram of the papermaking machine without any frame work is shown in Figure1.1.

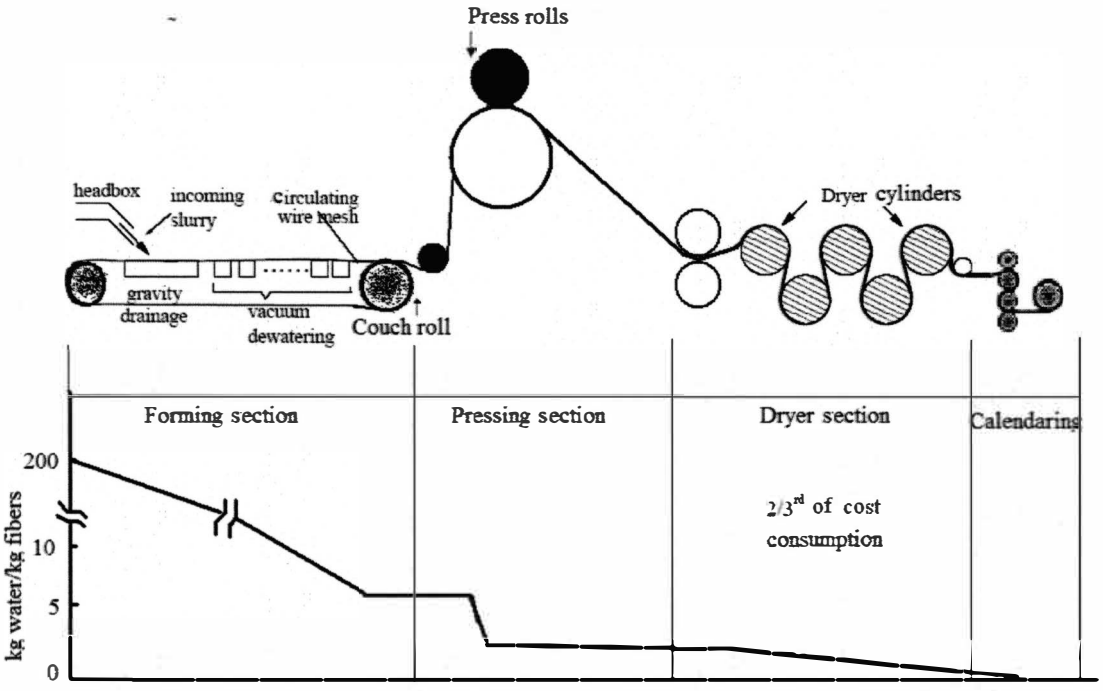

Figure 1.1 Water removals in a paper machine[1, 2]

The paper machine can be divided in four main sections. The first section is the forming section. Here, the water-fiber mix is sprayed out over the wire, a specially made net-like fabric. The purpose of the wire is similar to a filter: it allows the fiber to

consolidate, whereas excess water is free to pass through it. Most of the water leaves the pulp through the wire; however, there is still too much water left in the paper web to become paper. Web solids content can be increased in the forming section from less than 1% to about 13% to 30% by forces such as gravity, centrifugal force, hydraulic pressure between two fabrics, or vacuum created by drainage element or vacuum pumps[1].

Second is the press section. Here the paper web is pressed between two press rolls. Web solids content can be further increased by mechanical compression of the web in the press section. The press section is the most critical part in the paper machine because most paper properties depend on the performance of the press section. The key properties influenced by the press section are the surface and the strength of the final paper. The main surface properties affected are smoothness, caliper, and porosity. Influenced strength properties are tensile strength and tear strength[2].

The thru air drying (TAD) is widely accepted as the most effective drying method for increasing bulk and softness in commercial tissue production. Web compaction is reduced by avoiding wet pressing and this imparts the TAD sheet with up to 75% more bulk than a conventional dry crepe sheet of the same weight. The significantly reduced pressing load helps maintain the thickness of the sheet, producing a higher loft and more textured web. A better performance of the press section means less drying energy required in the drying section. In the press section, solids content can be increased by 3% to 15% depending on the performance of the press section. Today solids content of 50% is achieved on some of the paper machines in the press section. These machines have press sections equipped with shoe presses and impulse technology[2].

In the third section, known as the drying section, the remaining water is evaporated by letting the paper web come in contact with a large number of steam-heated cylinders. The number of steam heated cylinders can vary from 10 to 100 depending on the drying requirements[2].

The fourth section is the reel section (calendaring) where paper is given the final finishing and polishing touch. In this section, the paper is cut and rolled in desirable widths and lengths per requirements.

Normally, the wood pulp contains 166.6 tons of water for every ton of final paper produced, which are approximately 99.6% water and 0.4% solids. At the end of wire section paper has approximately 70% water and 30% solids and at the end of the drying section paper contains approximately 7% water and 93% of solids[4]. However, as the solids content of the wet web increases, additional water removal becomes more difficult, time consuming, and expensive in terms of both capital and operating cost[2].

Water remaining from the pressed sheet must be eliminated by evaporation in the dryer section. The paper drying in the dryer section is a slow and expensive operation. Two thirds of the total energy consumption for the paper machine is consumed in this section. Moreover Figure 1.1 illustrates how the mass of water removed in the dryer section is very moderate compared to the total dewatering capacity of an entire paper machine (Mc-Connell, 1980) as shown in reference 2. Therefore, great efforts have been put into optimizing performance of the press section. A small improvement of the pressing process can lead to higher solids content achieved before the drying section and significantly lowers the paper manufacturing cost. In general, an increase of one percentage point in the solids content yielded from the press section corresponds to a

4.5% decrease in dryer energy consumption per ton of final product[2]. Higher water dewatering rates can be achieved using a new web consolidation process: Rigid Capillary Dewatering.

Procter and Gamble Company has investigated the feasibility of using the rigid capillary dewatering (RCD) technology as a more cost efficient method for the removal of water from the fibrous web as a part of the paper making process. The paper machine with the RCD technology only differs in press section and all other sections are similar to conventional tissue making machine. The operating of this technology mainly uses the rigid capillary pressing roll (RCP).

RCD technology

Procter & Gamble Company has investigated the feasibility of using the RCD technology as part of the papermaking process. This technology is a novel web consolidation technique aimed to decrease investment costs and lowering the operational costs. The RCD is more cost efficient than conventional paper manufacturing processes for limited grades of paper[4].

It is the primary purpose of the press section to maximize water removal and simultaneously create the density potential required for desirable paper properties. Figure 1.2 and Figure 1.3 illustrate the construction of the press section with the RCD technology. The RCD process uses rigid capillary media and mild compressive action on fibrous web, that removes water from the fibrous web without excessive mechanical compacting of the fiber furnish. Vacuum box, located inside the RCP roll, and the limiting orifice medium (Figure 1.4), a mesh that covers the RCP roll, will improve the

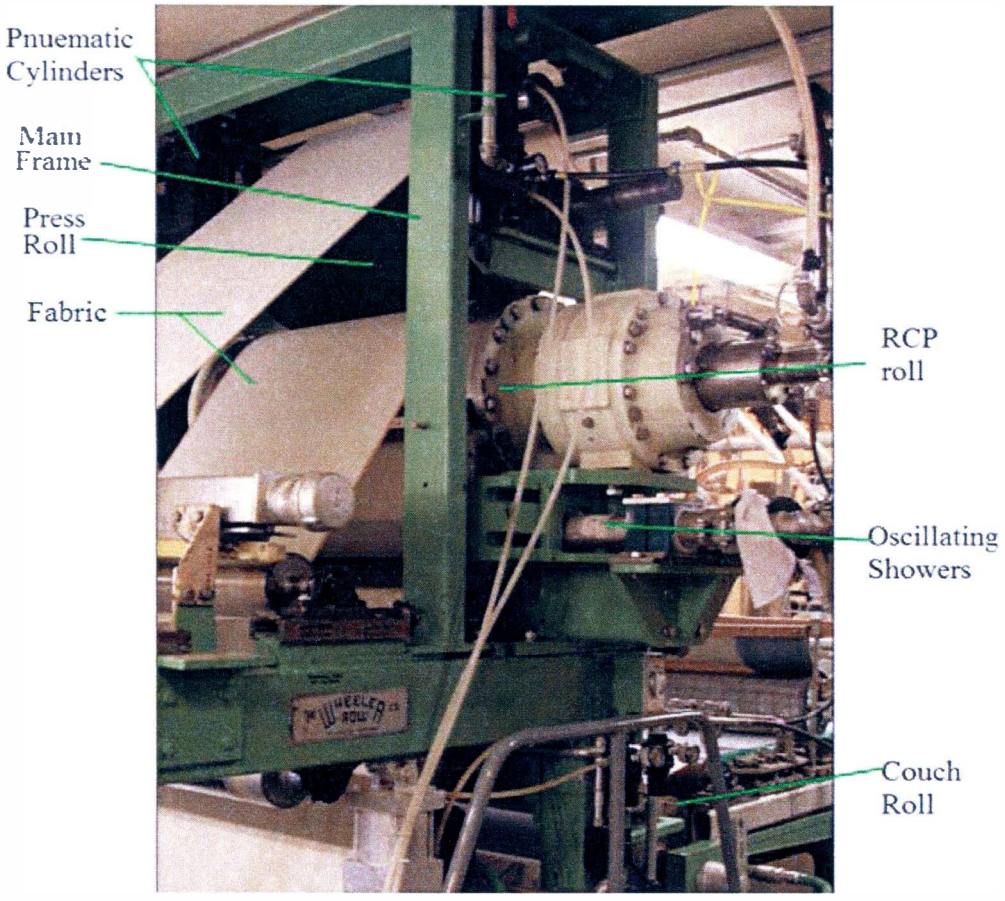

Figure 1.2 Actual construction of RCD press section

dewatering process by providing suction force. The press roll is also provided to apply press load during the dewatering process of the paper web.

Construction of press section

Framework

Figure 1.3 shows a mounting arrangement of the press section with the RPD technology which is similar to the press section of the conventional paper machine. The RCP roll is mounted on the main frame as shown in Figure 1.3. The press roll is mounted on the main frame above the RCP roll. The two pneumatic cylinders are attached to the

main frame, one on each end of the press roll. The pneumatic cylinders and the press roll are mounted on a pivoting frame. The pressure inside the pneumatic cylinders can be

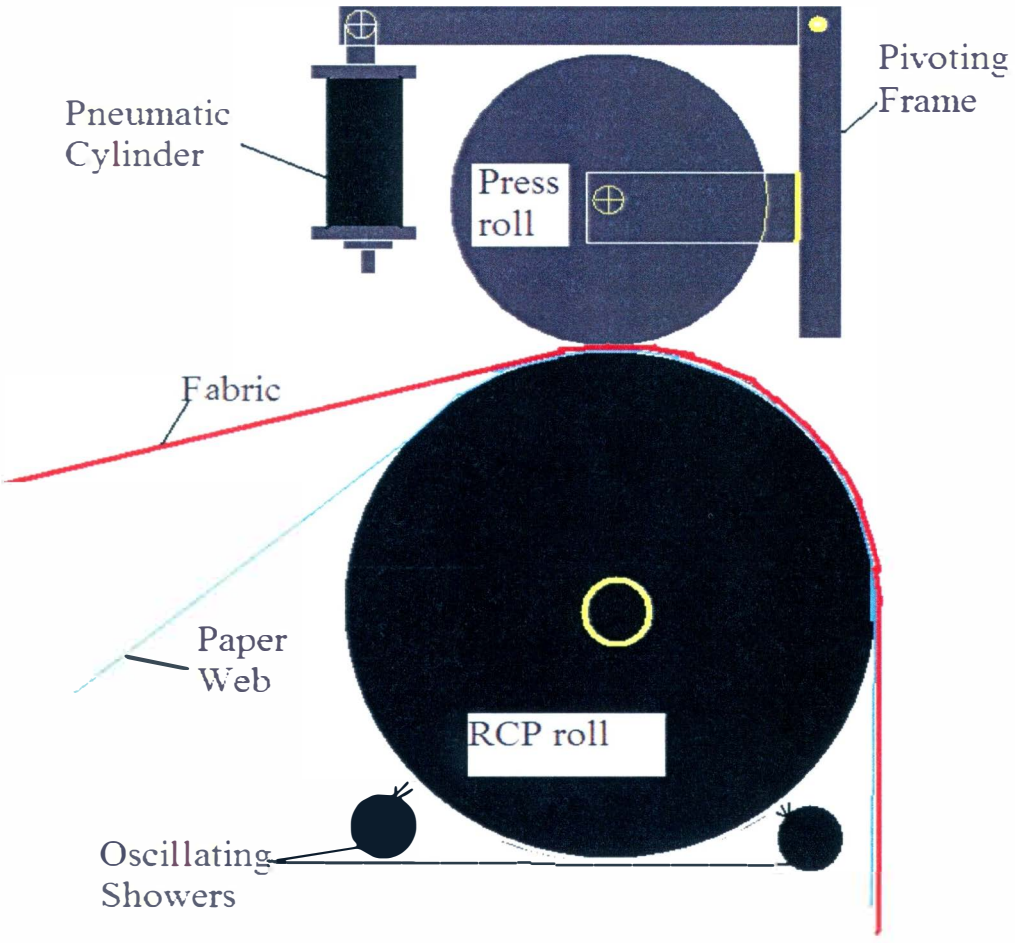

Figure 1.3 Sketch of construction of RCD press section

varied to adjust the press load. Two high pressure showers are mounted on the lower side of the RCP roll on the main frame, one on each side of the RCP roll. The high pressure showers are able to oscillate on the main frame for better performance. The fabric and paper web passes between the RCP and the press rolls. The paper web comes into contact with the RCP roll while the fabric makes contact with the press roll as shown in the Figure 1.3.

A 'nip point' or 'nip' is a localized point of contact between the press roll and the fabric. A nip pressure is the pressure between two rollers that are forced together. Nip impulse can be defined by ratio of nip load to machine speed[1]. A nip pressure is a measure of uniformity of that pressure. The application of a nip load increases hydraulic pressure and nip impulse, which drives water removal by increasing hydraulic pressure on the bottom side of the sheet.

Internal constructions of RCP roll[5]

The RCP roll is uniformly perforated cylinder with a pore diameter of 1.8 mm. Figure 1.4 shows internal construction of the RCP roll. The cylinder is covered with a specially manufactured mesh. There is a stationary suction box inside the RCP cylinder connected to a vacuum source. The suction box is open on the upper side and is supported by the sleeves, packing, and other seal holders. Low pressure showers are mounted adjacent to the suction box. The suction box remains steady irrespective of the rotation of the cylinder. The suction box can be rotated up to $\pm 15^0$ with respect to cylinder axis. The total open angle for suction box is approximately 165^0 and the remaining part of the cylinder is used by the shower zone and other supporting mountings inside the RCP cylinder. The pressure within the RCP roll for the suction box and low pressure showers are adjustable.

Limiting orifice medium

The limiting orifice medium (LOM) is comprised of a plurality of pores with fibrous web contacting and non-web contacting surfaces. The fibrous web is disposed on a supporting fluid permeable carrier (fabric) and the LOM; pressing the carrier and the

paper web between a pressing device and a LOM. The covering mesh of the RCP roll acts as LOM.

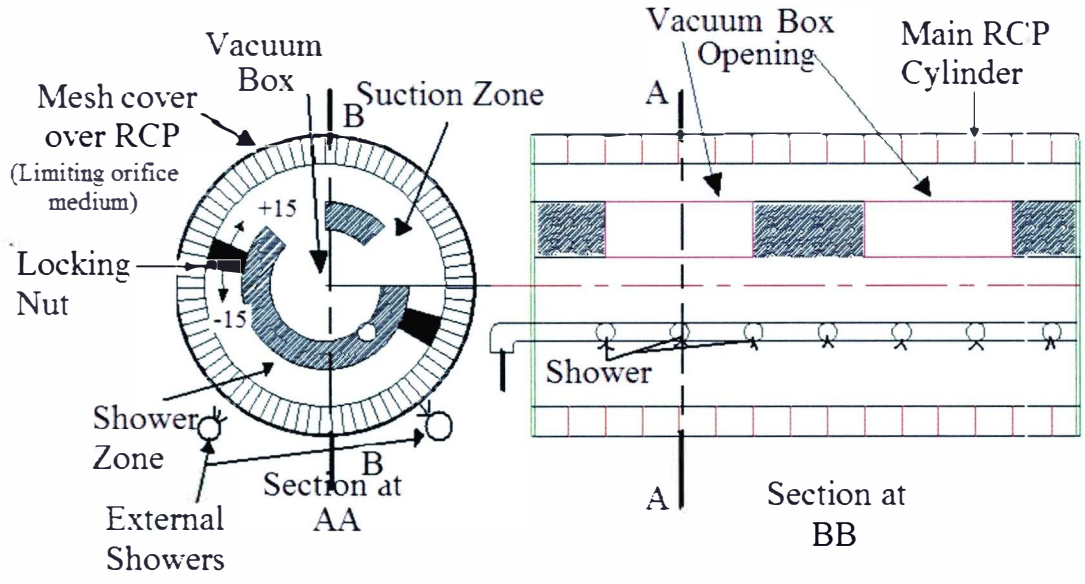

Figure 1.4 Internal construction of the RCP roll

The paper web is in surface contact with top layer of LOM. The capillaries in LOM are effectively smaller than the capillaries in the fibrous paper web, whereby some of water transferred from paper wet into LOM. The micro pores are well distributed to provide substantially uniform air flow to all of the fibrous structure. Alternatively, air flow through the LOM is influenced by providing a high resistance flow path (several turns, flow restrictions, small ducts, etc.) through the uniformly distributed micro pore medium[6, 7].

Figure 1.5 shows the covering mesh (LOM) of the RCP roll. The approximate thickness of LOM is 2 mm. The covering mesh is made with different sub layers having a pore size of 50 microns to 600 microns. The pore size and caliper (thickness) gradually

decreases from the inner layer to the surface. Each sub layer is specially woven mesh and calendared for better smoothness. The mesh construction is almost similar in warp and shute (perpendicular to warp) directions. In Figure 1.5, layer 1 has minimum pore size and caliper, while layer 5 has larger pore size and caliper. Layer 1 is in contact with the paper web and layer 5 is in contact with the RCP cylinder. The mesh cover is mounted on the RCP roll using shrink fit technology.

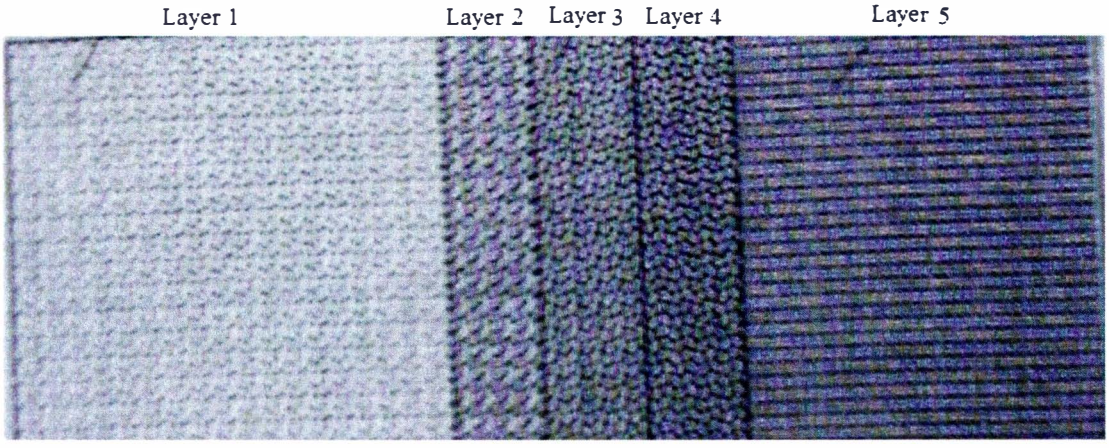

Figure 1.5 Limiting orifice medium[6, 7]

Figure 1.6 shows sketch of microstructure of layer 1. The pore size of the layer 1 is approximately 50 microns. Layer 1 is a Dutch Twill weave.

Breakthrough pressure

A sub-atmospheric pressure is a pressure less than one atmosphere of pressure. Such a pressure is also referred to as a negative, vacuum, or suction pressure. A breakthrough pressure is pressure when air flow begins through given media. The

moisture distribution in fibrous web is more uniform after air flow through LOM[6]. A 7 inHg of pressure is found out as breakthrough pressure for LOM over the RCP roll[8]. The

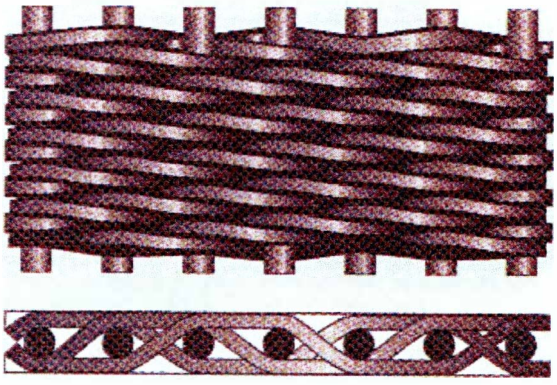

Figure 1.6 Layer 1, microstructure (dutch twill weave)

vacuum level is always kept above breakthrough level during dewatering of fibrous web through the RCP cylinder.

Principle of operation

The operation of the paper machine with the RCP roll is quite similar to a conventional paper machine except in the press section. After the forming section, the paper web will passed to the press section. The inlet solids content to the press section depends on the performance of the forming section. There is still a lot of moisture that needs to be removed after the forming section. The dewatering behavior of the paper web in the press section is defined by several important mechanisms. These mechanisms are due to the development of hydraulic and structural pressure gradients across the paper web thickness.

The operation of the RCP roll can be divided into three main zones: Zone-I at the beginning of vacuum zone, Zone-II at the press roll section, and Zone-III at the shower

zone as shown in Figure 1.7. The Zone I and II dewater the paper web while Zone-III cleans the cylinder surface for further operation.

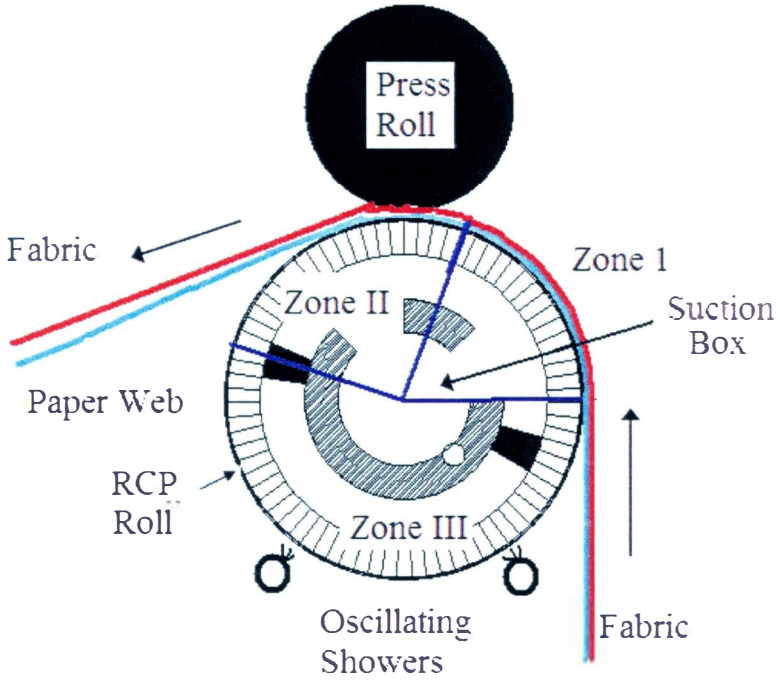

Figure 1.7 Press section operations

Firstly, the paper web comes from the forming section to the press section; it will come in contact with the RCP roll and the press section fabric. The dewatering of paper web begins at Zone-I. The applied vacuum in excess of breakthrough pressure of the pores of LOM results in the air flow through the fibrous web and into the pores. This movement entrains water in the web and either brings it into hydraulic contact with the pores, or carries it through the pores. The vacuum level is always maintained at breakthrough pressure or above[4].

In Zone-II, the mild compressive action, due to the press roll on the fabric at nip point, compact the paper web and more interstitial moisture is moved into hydraulic contact with the LOM. The applied vacuum in excess of breakthrough pressure on the

pores of the LOM and increased hydraulic contact of moisture further propagates the dewatering in Zone-II. After going through the press roll, the paper web is kept in contact with the RCP roll and the fabric is separated. After the Zone-II, the paper web is passed to the dryer section for further dewatering. As the RCP roll keeps rotating on its axis, it will come to Zone-III (shower zone).

There are possibilities that the fibers from the paper web have separated from the paper web and adhered to the micro pores of the LOM during dewatering in Zones I & II. The blockages of micro pores will prevent further fluid flow through them and progressively decrease the dewatering efficiency. Thus in Zone-III, the external high pressure showers mounted on the main frame clean the external surface and the internal low pressure showers clean the interior of the RCP cylinder. The absorbed water from the paper web and the water used by the internal showers are removed through the suction box. The cleaned cylindrical surface from Zone-III will come in contact with the paper web coming from the forming section again in Zone-I; where dewatering process continues.

The RCD process dewaters the paper web by rigid capillary action of LOM without significant pressing of paper web. Therefore it is not very effective on higher paper grades such as paperboard, writing paper and newsprint as they need higher sheet consolidation. The RCD process is effectively used for tissue and towel paper grades as these grades do not require higher paper web consolidation as they may destroy the required end usage characteristics. Therefore this thesis work concentrates mainly on the RCD technology behavior for lower paper grades such as tissue and towel paper grade manufacturing, which are less than 40gsm.

Rewet[1]

Rewetting (rewet) is one of the controversial aspects of wet pressing. Rewet is an effect rather that a variable in the strict sense and probably should be treated as negative water removal. The contact between the paper web and felt after the press nip causes rewetting of the paper web. Rewetting is shown in Figure 1.8. Rewetting is mainly due to the capillary forces which draw moisture from larger pores of the felt to smaller pores of fibrous web. Moisture transfer from the felt to the sheet is opposed by the centrifugal force acting on the water on the perimeter of the rotating press roll. Therefore, the external rewetting is more extensive on slow machines in which the opposing centrifugal force is small. The RCD technology uses fabric instead of felt which reduces rewetting. The amount of water transferred is independent of the basis weight. The low basis weight grades can therefore experience the largest decrease in percentage of the solids content.

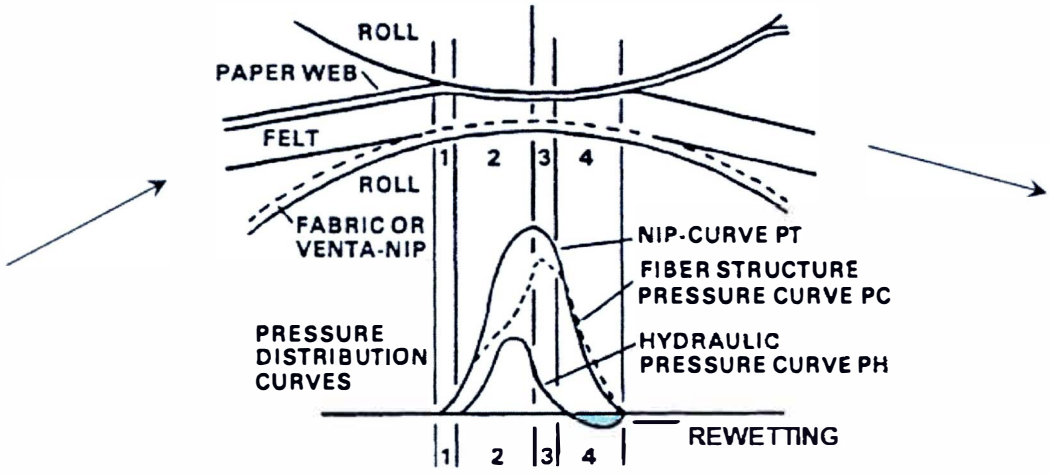

Figure 1.8 Rewetting phenomenon[9]

Various felt introduced rewet factors affect the sheet dryness by 2-7% and may be more[1]. For example, external rewet can decrease the solids content of newsprint by as

much as 3%. In the RCD process, the compressible felt is replaced by the incompressible capillary media (fabric). Thus at constant press parameters, the RCD process can improve the after press sheet dryness by 2-7+% depending on the paper grade by eliminating the felt introduced rewet phenomena[4].

Advantages of the RCD technology

There are four main advantages of RCD technology as discussed below:

(1) Reduced dryer section energy usage[2]:

The RCD technology reduces the moisture content of the paper web that needs to done in more expensive dryer section. In general, an increase of one percent in solids content exiting the press section corresponds to the 4.5% decrease in the dryer section's energy consumption per ton of final product.

(2) Increased paper productivity for drying limited grades[1]:

The RCD technology has limited capillary suction capability, thus it is not very effective on higher grade papers such as paperboard, writing paper and newsprint. However, the RCD technology has very good dewatering capability for paper with 20gsm to 70gsm basis weight without destroying required end product characteristics.

(3) Improved strength properties of paper:

During drying, the diameter of swollen fibers is reduced and, consequently, the fiber network also tends to shrink[10]. When paper is dried without restraint, its tensile strength is not fully developed, but it exhibits larger strength to rupture and usually absorbs more energy before

rupturing. Due to very mild pressing action in the RCD technology, the inner fiber structure of paper web is minimally damaged. This fiber structure exhibits lower strength properties due to weak bonding between fibrous structures required for tissue and towel grades of paper.

(4) Improved bulk, softness, handle and fluffiness of the paper:

The RCD technology dewaters the paper web with the RCD action and not with impulse action. The RCD action applies very mild compression on the paper web, and air voids are created in paper web during dewatering. The air voids created during the RCD dewatering enhances bulk, softness, handle, and fluffiness of the paper for given basis weights. The paper is made on a very smooth surface just before entering the dryer section will result in improved paper smoothness on the side pressed against the roll[1].

Chapter previews

There are many parameters which affect the performance of the RCD technology. Chapter II discusses the parameters that affect the machine performance. Parameters affecting the dewatering process are divided into three main categories, which are the paper properties, the pulp properties, and the machine operating parameters.

Chapter III shows experimental procedure carried for experimentation. Further Chapter III shows discussion of all experimentation carried out and results obtained during study of the RCD technology at Western Michigan University (WMU) paper pilot plant facility.

There are many forces that govern the dewatering mechanism of the paper web. Chapter IV shows individual effects of forces acting in terms of their magnitude. The mathematical model for capillary rising is solved and validated by comparing results with reference work. Further, Chapter IV discusses the mathematical model development for capillary dewatering as done in reference work under the forces governing dewatering in RCD technology. The mathematical model is developed and solved to understand the dewatering behavior of the RCP roll.

Chapter V discusses the conclusions observed from the results obtained during experimentation of the RCD technology at WMU paper pilot plant facility. Chapter V also discusses the conclusion for results obtained from mathematical model. Further Chapter V shows possible research areas needs to work on for further development in the RCD technology.

CHAPTER II

EXPERIMENTAL PARAMETERS

We have seen the background, construction, and the working principle of the RCD technology. The RCP roll is mounted in the press section and the paper web is forwarded to the RCP roll after the couch roll of forming section. This chapter will show behavior of the RCP roll under given operating parameters. The paper web contains 20 - 25% solids at the end of the forming section for the WMU pilot paper machine. The paper web leaving the RCP roll contains 25 - 35% solids depending on the performance of the RCP roll. The final consistency will depend upon the incoming moisture, fiber composition, the Canadian Standard Freeness (CSF) of the pulp furnish, the basis weight of web, the pressing pressure in the nip, the residence time of the web on the LOM, and the functional pores size of the LOM[6]. The extent of drying in the RCD is also dependent upon the moisture saturation, flow rate, and temperature of air flowing through the paper web[6]. Performance of the RCP roll can be determined in terms of different paper properties and in terms of different operating conditions in the press section.

Operating parameters for the RCD

The discussion is divided into three sections:

1. Paper properties
2. Pulp properties
3. Operating parameters of machine

Paper properties

Basis weight / grammage[1, 12]

The "basis weight" or "grammage" is a fundamental property of the paper that measures weight per unit area. The weight, measured in pounds, of 500 sheets (a ream) of paper cut to a standard size is its basis weight. The basis weight is important from the point of view of production rate. For tissue, the basis weight ranges from 20-40GSM (gram per square meter) or 12 – 25 lb/3000ft^2. The RCP roll is not very effective for higher basis weights because a higher vacuum level and lower machine speed is required.

Caliper

Caliper refers to the nominal thickness of a sheet of paper. Caliper is measured in mils for paper, which are expressed in thousandth of an inch[1]. Caliper is defined as the particular distance between the two principle surfaces of the paper or paperboard under prescribed conditions. This measurement is taken with a micro meter. Normally, paper caliper should not have more than a $\pm$5% variance within a sheet. Variations in a caliper can affect several basic properties including a strength and paper roll quality. The RCP roll dewaters the paper web by the RCD action and nominal compression forces which prevent the paper sheet from becoming denser. Therefore, the paper with the same basis weight made on the RCP roll has higher caliper compared to that of conventional techniques.

Moisture content (water-fiber ratio)

Moisture content of the paper is expressed in percentage of moisture of the given paper grade[11]. All grades of paper have some percentage of moisture. Moisture content can be measured with the use of microwave oven or hot plate and a scale. Moisture content in the paper varies from 2 - 12% depending on relative humidity, grade of paper, type of pulp, degree of refining, and chemicals used[1]. Most of the physical properties of paper show variation as a result of variations in moisture content. Moisture control is also significant from the economic aspect of paper making. The performance of the RCP roll can be estimated by measuring difference between moisture content of paper web before and after the RCP roll. Moisture content before the RCP roll is 75 – 80% and after the RCP roll is 80 – 65%. The difference will give the dewatering efficiency of the RCP roll under given conditions. A higher moisture content difference represents a better performance of the RCP roll. Moisture difference of 1 -15% can be obtained depending on operating conditions of the RCP roll.

The performance of the RCP roll can be measured in terms of moisture removal rate. Moisture content can be found in terms of pound of water per pound of fibers present in paper. The paper samples before and after the RCP roll are taken and moistures content are measured. Difference between the moisture content is expressed in 'lb/lb'. The lb/lb stands for pound of moisture per pound of fibers.

Porosity

Porosity is a structural property of the paper. Porosity is a measurement of total connecting air voids, both vertical and horizontal, that exist in a sheet through which

fluids may pass[11]. Porosity can also be defined as the compactness of the fibers in the paper. Porosity can be measured with a permeability tester[3]. Porosity of a sheet is an indication of an ability of the sheets to accept fluid. Paper is a highly porous material and contains as much as 70% air. Because paper is composed of a randomly felted layer of the fibers, the structure has a varying degree of porosity. Porosity also depends on the type of applied press action at the press section. The RCP roll mainly uses the RCD action and mild mechanical pressing for dewatering; the paper web is dried without restrain of the fibers[1]. Thus, paper made by the RCD method has higher air voids in paper web and high porosity compared to the paper made by the conventional paper making process.

Tensile[11]

Tensile is a strength property of the paper. Tensile strength is the force required to produce a rupture in a unit width of the paper strip. Tensile strength can be measured with a universal testing machine. The tensile strength should be measured in machine and cross machine direction and expressed in kN/m. Tensile strength depends on fibers bonding, fiber densification, and fiber length of paper pulp. The RCD technology applies mild mechanical pressing, therefore the internal fiber structure is not strained during dewatering. When paper is dried without restraint, its tensile strength is not fully developed, but it exhibits larger stretch to rupture and usually absorbs more energy before rupturing.

Tearing resistance

The tearing resistance is a measure of the work required when a test specimen of the paper is torn through a specified distance[11]. Based on the total work required, the force required to propagate the tear can be calculated and is expressed in mN. Fiber length and inter-fiber bonding are important factors for tearing strength. The fact that longer fibers improve tear strength is well recognized. The explanation is straight forward; longer fibers tend to distribute the stress over a greater area, over more fibers and more bonds, while short fibers allow the stress to be concentrated in a smaller area[3]. The RCD technology applies mild press loading action, which dewaters the paper web without breaking internal fiber bonds. Therefore, papers made using the RCD technology have better tearing resistance.

Pulp properties

Type of fibers

There are mainly two types of fibers, hardwood fibers and softwood fibers. Hardwood fibers are generally 1-3 millimeter long and 20 micrometer thick. Softwood fibers are 2-7mm long and 20-30 micrometer thick. Hardwood fibers give good softness, smoothness, and low strength properties to paper. Thus, hardwood fibers are especially suited for producing smooth papers. Hardwood fibers also tend to produce paper products with more uniform formation. Softwood fibers confer tearing strength, tensile strength, and ability to withstand multiple folding[3].

Refining

The word "refining" is often used as a synonym for "beating." Both words refer to the passage of pulp between the rotor and stator in housing, or counter-rotating disks. Raised areas of bars on the rotor and stator expose the fibers to repeated compression and shearing forces. These forces gradually delaminates the fiber cell wall, increasing flexibility and fibrillation of the fiber surfaces. During the refining, the cell walls are partially delaminated resulting in a microscopically hairy appearance of the wetted fiber surface. This enhances strength of fiber of fibers bonds[3]. The refining degree is varying from 700 – 100 CSF (Canadian Standard Freeness). The 700 CSF indicates unrefined pulp.

Operating parameters of machine

Vacuum level

The pressure below the atmospheric pressure is known as sub-atmospheric, vacuum, negative, or suction pressure. The vacuum level is measured by a pressure gauge mounted on the suction line. The special design of the mesh covering the RCP roll creates the LOM which is helpful in maintaining pressure inside the RCP roll. The application of a negative pressure in excess of breakthrough pressure across the LOM will result in the air flow through the paper web to the pores[4]. Therefore, the pressure above breakthrough will give some air flow and dewatering will take place. Pressure below breakthrough will not create any air flow through the RCP roll. For the given RCP structure, 7 inHg of

pressure has been determined to be the breakthrough pressure by previous experiments[7]. Therefore, the vacuum level should be sustained above 7 inHg for dewatering.

Press load

The press roll exerts a pressure on the fabric above the paper web. This pressure is opposed by the mechanical pressure of the paper web fibers and the hydraulic pressure of the fluid contained in the paper web. Due to mild compression of the paper web, the total hydraulic pressure increases over the RCP roll without significantly straining the internal fibrous structure of paper web. Uniformity along the line of pressure of the press roll on the fabric is also a very important factor in the RCD technology. Non-uniformity along the line of pressure of press roll will not result in uniform dewatering.

The press load can be measured in 'pli', i.e. 'pound per linear inch'. The press load is applied due to weight of the press roll itself and two pneumatic cylinders attached to the pivoting frame over the press roll as shown in Figure 1.3. The press load can be changed by varying the pressure inside the pneumatic cylinders. The pressure in each of the cylinders should be kept equal all times. The facility at Western Michigan University (WMU) paper pilot plant has a range of 0 – 40psi load in pneumatic cylinders. The pressure is converted to pli as shown below,

Force out of cylinders (F_c) = Cylinder pressure (psi) X Area of cylinder X No. of cylinders

Effective force (F_{ceff}) on the roller can be given as follows:

$$F_{ceff} = (F_c \times L_{proll}) / L_{fabric}$$

$$\text{Nip Load (pli)} = (F_{ceff} + W_{roller}) / W_{paper}$$

Machine speed

Machine speed is defined by the paper production speed. It is derived in terms of m/min or ft/min. Machine speed can vary between 30 fpm to 2500 fpm. As speed is increased, water removal from the sheet will decrease with other conditions held constant for wet press[1]. The RCP roll's speed determines the total contact time between the paper web and the suction zone of the RCP roll. The total contact time between the suction zone and paper web should allow enough time for fluid to flow from the paper web through the LOM. A higher machine speed allows less contact time between paper web and the suction zone, causing higher uncertainty in the press load. Higher machine speed also increases the centrifugal force acting on the fluids in the LOM and in the paper web. Thus, to make dewatering more effective, roll speed should allow enough contact time between the paper web and suction zone to make a uniform press load distribution over the paper web.

Sheet breaking

Sheet breaking is the main runnability issue in the RCD trials. Figure 2.1 shows paper web breaking locations while conducting the RCD trial run.

Sheet breaking arises because paper web has a low strength of paper web, uncertainty in press loading, and poor pickup after the forming section and the press section. To improve the runnability of paper web, the suction box was assembled on the side of the fabric between the couch roll and the RCP roll. This allowed better pickup of the paper web after the couch roll. The suction box arrangement is shown in Figure 2.2. This idea is successful to some extent for lower machine speeds.

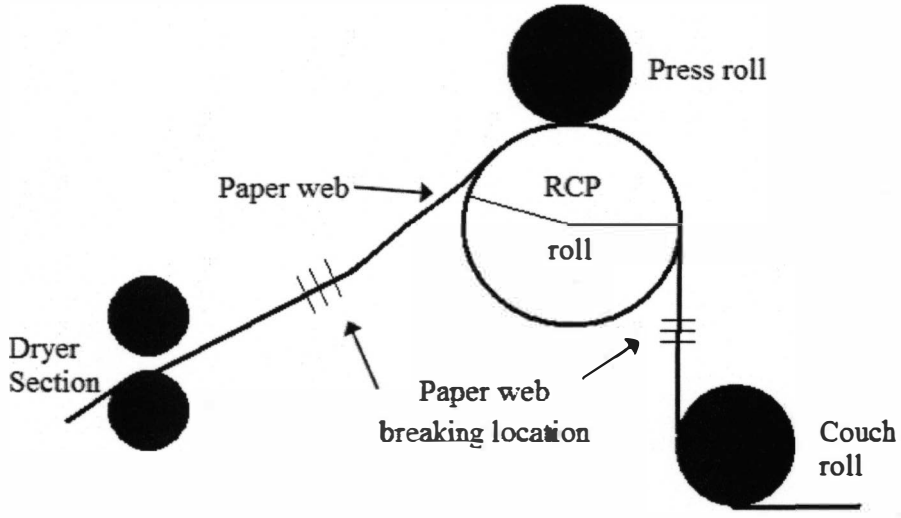

Figure 2.1 Sheet breaking

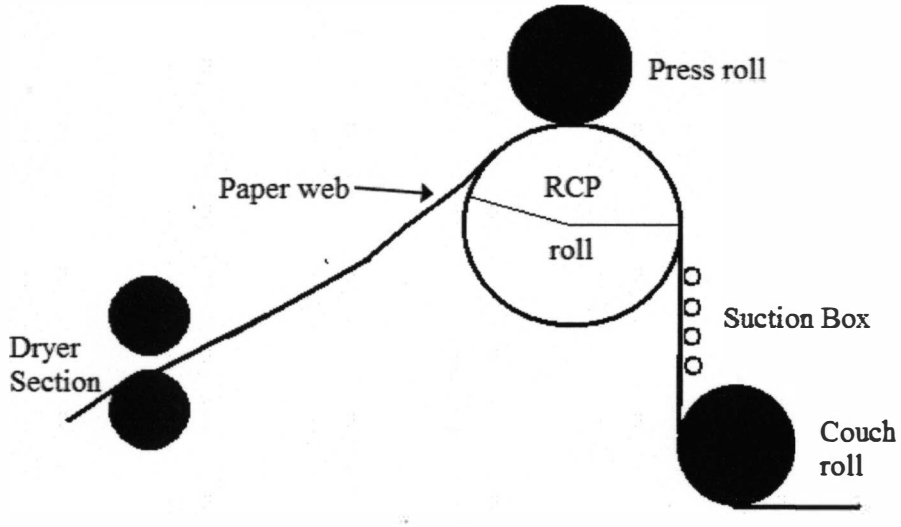

Figure 2.2 Suction box arrangement

The sheet breaking is also reduced by improving sheet strength. The sheet strength can be improved by further lowering the CSF and by creating a higher content of softwood fibers in wood pulp. For example freeness of 350CSF will give better runnability compared to 650CSF pulp.

CHAPTER III

EXPERIMENTATION

Experimental procedure

The pulp is prepared with desired mixture of softwood and hardwood fibers and refined up to the desired freeness. Then, the paper making machine is prepared for a trial run. The machine preparation is similar to that of conventional machines. Firstly, the machine is washed and all the joints and connections are checked. Additionally, the dryer rolls from dryer section are heated up using the steam supply.

The paper machine runs as discussed in the Chapter I. During the machine run, the operating variables are changed as per the test requirements and samples are collected. The piece of the paper is taken out by hand and kept in airtight plastic sample bags. Required numbers of paper sample are collected, before and after the RCP roll, for further testing.

The paper sample is tested using the proper methods and the TAPPI (technical association of the pulp and paper industry) standards for given test. The table below shows ranges for different operating parameters important for a paper trial run.

Table 3.1 Paper trial run limit estimations for WMU pilot paper machine.

Sr.No.*	Variables	Range		Unit
1	Machine speed	40	80	Fpm
2	Press load	20	65	Pli
3	Basis weight	30	60	3000 lb/ft^2
4	Vacuum level	0	14	inHg
5	Internal Showers	On	Off	
6	Freeness	700	250	CSF
7	Pulp Type	90% SW** & 10% HW***	10% SW** & 90% HW***	%

Sr. No.*: Serial number
SW**: Softwood
HW***: Hardwood

Based on the limits for given variables as shown in Table 3.1, four experiments were carried out. The details of experiments are shown further.

Trial #1

February 17, 2006

Furnish: 90% southern softwood, and 10% southern hardwood

Effects of four RCD operating parameters were investigated in this test. These are:

- Freeness: 562 CSF and 323 CSF
- Vacuum level: 10 inHg and 14 inHg
- Press load: 16pli, 33pli, and 48pli
- Basis weight: 65 lb/3000ft^2 and 45 lb/3000ft^2

This trial began with unrefined (700CSF) 90% southern softwood and 10% southern hardwood furnish. In this trial we were not able to run it consistently. Sheet couching was the severe problem because sheet kept breaking between the couch roll and the RCP roll.

To improve the functionality of the trial, the pulp was refined to 650CSF and then to 562CSF. Later on, the trial pulp was refined further and freeness reduced to 323CSF. In order to reduce the sheet breaking, the vacuum source was attached to the fabric in between the couch roll and the RCP roll as shown in Figure 2.1. The vacuum source was taken from the main suction source (suction box).

This trial was helpful to find relation of solids content with press load and machine speed. This trial was also helpful in finding relation of press load with caliper, porosity, tensile strength, and tear strength for a given furnish of pulp.

Results Trial #1

Available results for Trial #1 are summarized in Table 3.2. Based on these results, following relations can be obtained. Results show better dewatering ability for lower basis weights and higher machine speeds.

Figure 3.1 show approximately 75% increase in change in solids content for approximate 100% increase in press load for some extent and then change in solids content gradually reduces for higher press loadings. Based on results, 33pli pressing load increases the water removal on the RCP roll by 0.34 lb/lb water compared to 16pli press load.

Table 3.2 Dewatering results for furnish 90% southern softwood, and 10% southern hardwood.

Sr. No.	Free-ness	Basis weight	Vacuum level	Press load	Machine Speed	Solid content		Change in Solid content	Moisture removal	Porosity		Caliper	Tensile Strength		Tear Strength	
						BRCP+	ARCP++			Smooth side	Rough side		M/c Dir.	C/s Dir.	M/c Dir.	C/s Dir.
	CSF	lb/3000ft²	InHg	pli	fpm	%		%	lb/lb	ml/min		1/1000 inch	kN/m		mN	
1	650	63	14	48	54	22.5	23.6	1.1	0.65							
2	562	63	14	48	54											
3	562	61	14	48	55	21.1	22.9	1.8	1.03	9407	9779.2	9.712	2.46	1.7	1893	1922
4	562	67	14	48	55											
5	562	67	14	48	55											
6	562	57	10	48	55											
7	323	54	10	29	55	21.37	24.39	3.02	1.53	4645	4455	9.825	5.33	2.31	1874	2358
8	323	53	10	32	55	21.66	24.8	3.14	1.56							
9	323	47.9	10	48	63	20.16	25.22	5.06	2.28	4042	4261	8.66	4.62	4.22	1515	1736
10	323	41.5	10	48	67	20.28	25.3	5.02	1.96							
11	323	41.5	10	48	71	20.58	24.9	4.32	1.69	4273	3892.5	7.737	4.96	2.22	1340	1751
12	323	40	10	33	71	19.2	24.59	5.39	2.03							
13	323	40.6	10	16	71	20.06	23.06	3	1.14	5636	5953	7.333	5.01	1.97	1251	1622

BRCP+ Before RCP roll
ARCP++ After RCP roll

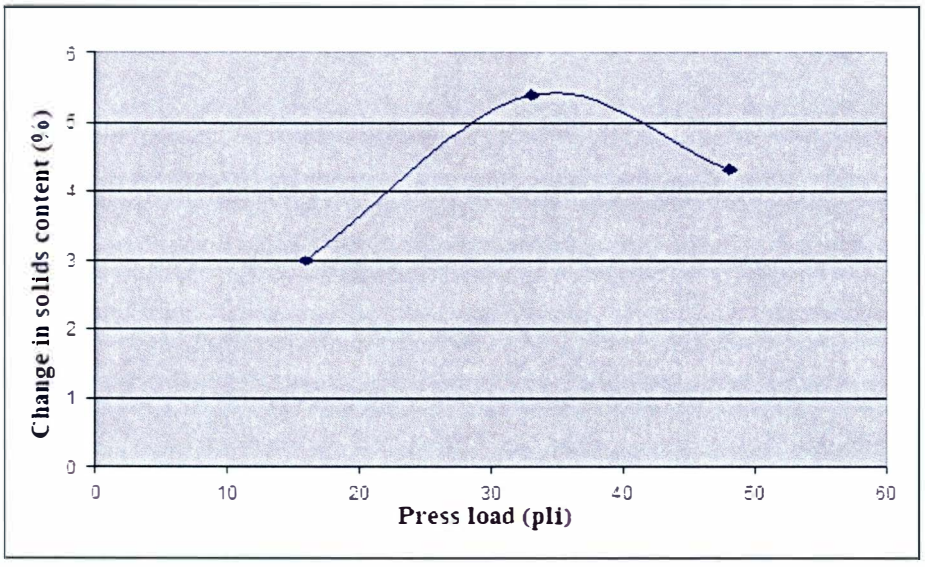

Figure 3.1 Change in solids content vs. press load (constant basis weight)

Figure 3.2 shows decrease in change in solids content for increase in machine speed for given vacuum level. Figure 3.2 shows 15% decrease in solids content compared to 13% increase in machine speed. Change in solids content is higher for lower machine speeds.

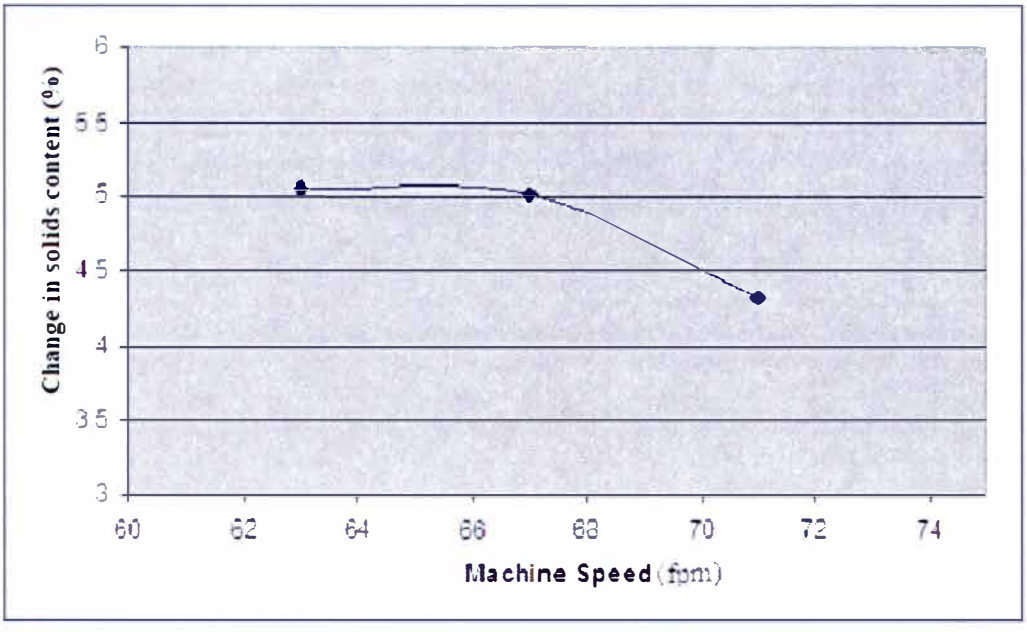

Figure 3.2 Change in solids content vs. m/c speed (constant vacuum level)

However, water removal rate is higher for higher machine speed. Water removal rate is approximately 1 lb/lb for machine speed of 50 fpm and approximately 2 lb/lb for machine speed of 70 fpm.

Figure 3.3 shows caliper remains almost similar for up to 300% increase in press load. This shows the applied press load is not affecting the caliper of the paper web.

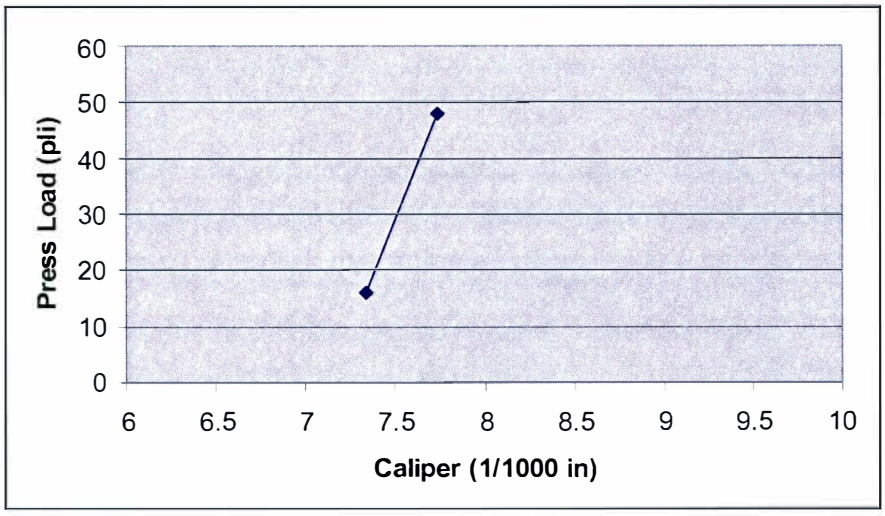

Figure 3.3 Press load vs. caliper (constant basis weight and m/c speed)

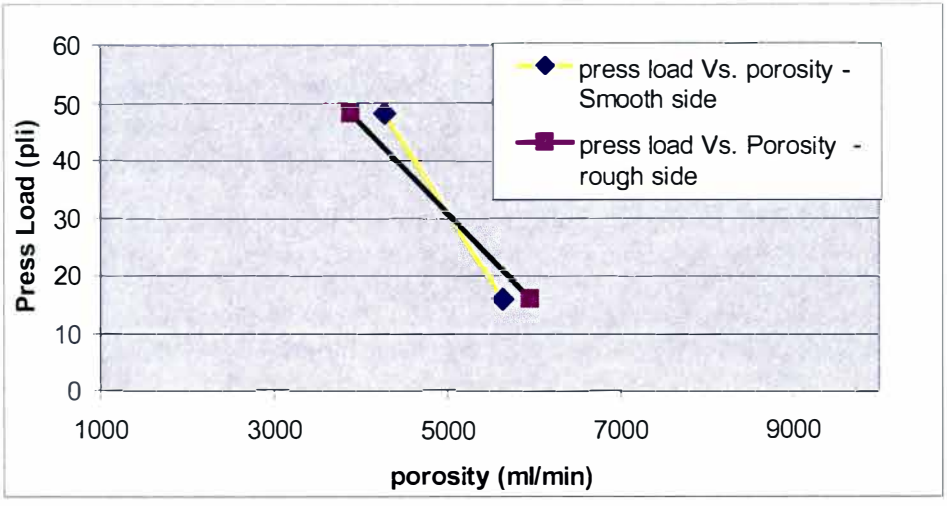

Figure 3.4 Press load vs. porosity (constant basis weight and m/c speed)

Figure 3.4 shows 50% decrease in porosity for 300% increase in the press load. Thus pressing action in the RCD technology is significant on the porosity.

Figure 3.5 shows increase in tensile strength with increase in press load. The increase in tensile strength with respect to increase in press load is not significant because there is only 10% increase in tensile strength for 300% increase in press load.

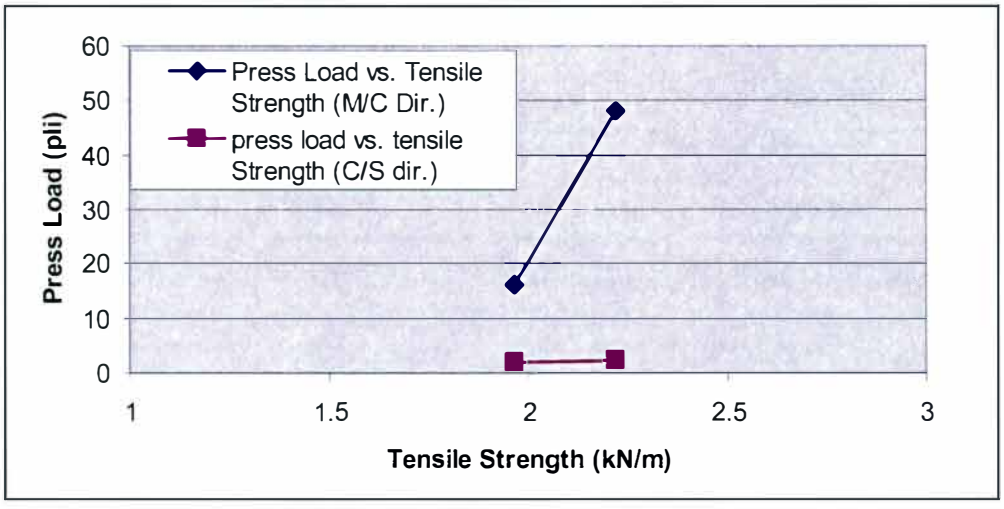

Figure 3.5 Press load vs. tensile strength (constant basis weight and m/c speed)

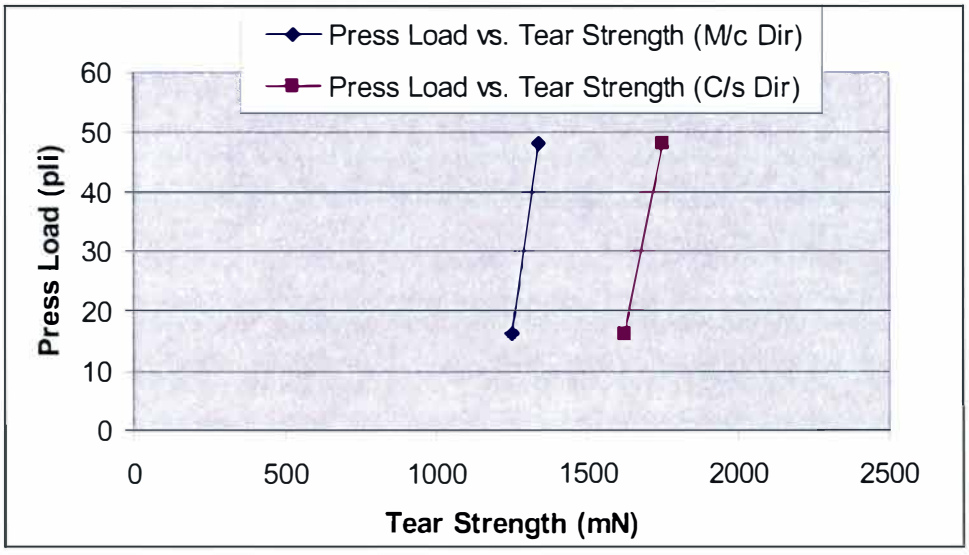

Figure 3.6 Press load vs. tear strength (constant basis weight and m/c speed)

Figure 3.6 shows tear strength increases for increase in press load. There is approximately 7% increase in tear strength compared to 300% increase in press load. Therefore, press load is not significant on tear strength of paper web.

Trial #2

March 16, 2006

Furnish: 10% southern softwood, and 90% southern hardwood

Trial #2 ran the same parameters as were run in Trial #1 with different fiber furnish. The Trial #2 was not successful; the press load pulley was jumping during the machine run. The pulley was jumping because of improper gear belt, driving the motor and press roll. To avoid any damage to the RCP roll the trial was canceled.

Trial #3

March 28, 2006

Furnish: 40% southern softwood and 60% southern hardwood

The effects of the RCD operating parameters were investigated in this test. These are:

- Vacuum level 0 inHg, 5 inHg, 10 inHg.
- Press load, 16pli to 59pli.
- Internal shower condition: On/Off.

This trial was mainly performed to check the machine stability after replacing the gear belt. This trial includes the variation of change in the solids content with the shower condition for a given basis weight. This trial also shows the relation of change in the

solids content with the vacuum level and the press load for a given basis weight and fiber furnish.

This trial started with 450 CSF 40% southern softwood with 60% southern hardwood furnish. In this trial we were not able to run it consistently and again sheet couching was the problem. Sheet kept breaking between the RCP roll and the dryer section. Therefore, the trial was limited to the press section and samples were collected only before and after the RCP roll.

Results Trial #3

Table 3.3 Dewatering results at 72.9 fpm and freeness = 450CSF.

Sr. No.	Internal shower condition	Basis weight	Press load	Vacuum level	Consistencies, %		Change in solids content	Moisture removal
		Lb/ 3000ft^2	pli	in Hg	BRCP	ARCP	%	lb/lb
1	On	37.4	16	10	21.5	34.85	13.35	4.69
2	On	37.4	26.62	10		33.85	12.35	4.34
3	On	37.4	37.36	10	21	35	14	4.92
4	On	37.4	48.1	10		35.77	14.77	5.19
5	On	37.4	58.83	10		34.55	13.55	4.76
6	Off	34.4	37.36	5		28.93	7.93	2.56
7	On	34.4	37.36	5		29.22	8.22	2.66
8	On	34.4	37.36	5		27.57	6.57	2.12
9	Off	34.4	26.62	5		22.34	1.34	0.43
10	Off	34.4	37.36	0		21.26	0.26	0.08
11	Off	34.4	16	5		17.9	-3.1	-1.00
12	On	35.5	37.36	5	21.8	18.86	-2.94	-0.98
13	Off	35.5	37.36	0		20.27	-1.53	-0.51
14	Off	35.5	26.62	0		20.13	-1.67	-0.56
15	On	35.5	48.1	5		17.7	-4.1	-1.37

Results are summarized in Table 3.3. Based on these results, following relations can be obtained. Figure 3.7 shows significant increase in change in solids content for

increase in vacuum level for given press load. Based on the previous results, 7 inHg is the break through pressure and for better performance of the RCP roll the vacuum level should be maintained above break through level[8]. Figure 3.7 shows the similar behavior, better dewatering for pressure above breakthrough level and low dewatering efficiency for pressure below breakthrough level.

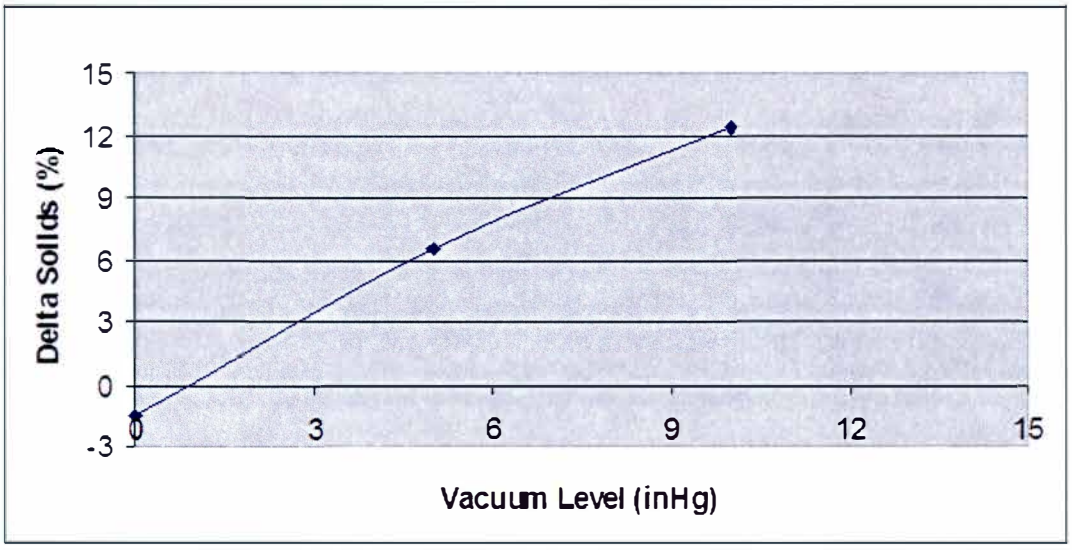

Figure 3.7 Change in solids content vs. vacuum level
(constant press load, m/c speed, and basis weight)

Figure 3.8 shows dewatering behavior of paper web for varying press loads. Change in solids content of the paper web increases for certain value of press loads and after reaching peak dewatering decreases for higher press loads. Water removal rate also increases for certain value of press loads and after reaching peak water removal rate decreases for higher press loads.

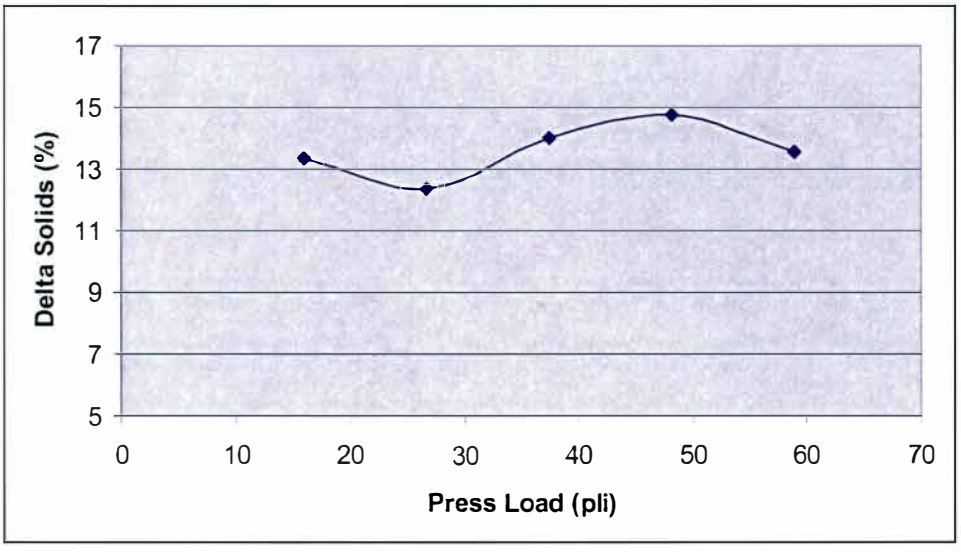

Figure 3.8 Change in solids content vs. press load
(constant basis weight, m/c speed, and vacuum level)

Trial #4

July 17, 2006

Furnish: 40% southern softwood, and 60% southern hardwood.

Freeness = 450CSF

Effects of the four RCD operating parameters were investigated in this test. These are:

- Vacuum level 0 inHg and 10 inHg.
- Press load, 16pli, 26pli, 37pli and 48pli.
- Basis weight 42 lb/3000ft^2, 35 lb/3000ft^2.
- Internal shower condition, On/Off.

The primary purpose of this trial was to replicate the previous trial's results and ensure the consistency of machine performance. This trial started with 450CSF and 40% southern softwood and 60% southern hardwood furnish.

This trial was successful and relationships between change in solids content with the press load and the vacuum level were obtained for the given furnish of pulp.

Results Trial #4

Table 3.4 Dewatering results at 72.9 fpm and freeness = 450CSF.

Sr. no.	Internal shower condition	Basis weight	Press load	Vacuum level	Consistencies, %		Change in solid contents	Moisture removal
		lb/ 3000ft^2	Pli	inHg	BRCP	ARCP	%	lb/lb
1	On	35	26.6	10	21.3	31.85	10.55	3.47
2	On	35	16	10		32.62	11.32	3.72
3	On	35	16	10		33.3	12	3.95
4	On	35	37.4	10		31	9.7	3.19
5	On	35	48.1	10		33.01	11.71	3.85
6	On	35	37.4	8		32.1	10.8	3.55
7	Off	35	16	0		20.4	-0.9	-0.30
8	Off	35	26.6	10		25.2	3.9	1.28
9	Off	35	37.4	10		34	12.7	4.18
10	On	42	16	10	21.11	33.6	12.49	4.93
11	On	42	26.6	10		34.5	13.39	5.29
12	On	42	37.4	10		35.4	14.29	5.64
13	On	42	48.1	10		34.3	13.19	5.21
14	Off	42	37.4	0		21.32	0.21	0.08
15	Off	42	37.4	10		26.5	5.39	2.13

Results for Trial #4 are summarized in Table 3.4. Based on these results, following relations can be obtained.

First observation shows (results #8 and 9) significant increase in change of solids content for increased press load for basis weight 35 lb/3000ft^2 and internal shower off. Increase of 26.6 pli to 37.4 pli press load approximately increases 2.9 lb/lb of water removal.

Second observation shows dewatering behavior of basis weight 35 lb/3000ft^2 for pressure above breakthrough level and internal shower kept on gives approximately 3.2 to 3.8 lb/lb water removal.

Third observation shows significant increase of approximately 3.51 lb/lb water removal depending on shower situation for given press load, basis weight, and vacuum level as shown in obtained 12 and 15. Change in solids content is significantly changes from 5.39% to 14.29% for off to on condition of internal shower.

Forth observation shows higher dewatering ability for higher basis weight. Basis weight 42 lb/3000 ft^2 shows better dewatering compare to basis weight 35 lb/3000 ft^2. Table 3.4 shows increase of approximately 2lb/lb water for higher basis weight.

Figure 3.9 shows dewatering behavior of paper web for varying press loads for different basis weight. Change in solids content of the paper web increases for certain value of press loads and after reaching peak dewatering decreases for higher press loads for 42 lb/3000ft^2 basis weight. Change in solids content of paper web decreases for certain value of press loads and after low down it increases again with increase in press load for 35 lb/3000ft^2. Change in solids content increases for increase in press load for 35 lb/3000ft^2 with shower off.

Observation in Figure 3.10 shows better dewatering for pressure above breakthrough level and lower dewatering efficiency for pressure below breakthrough level.

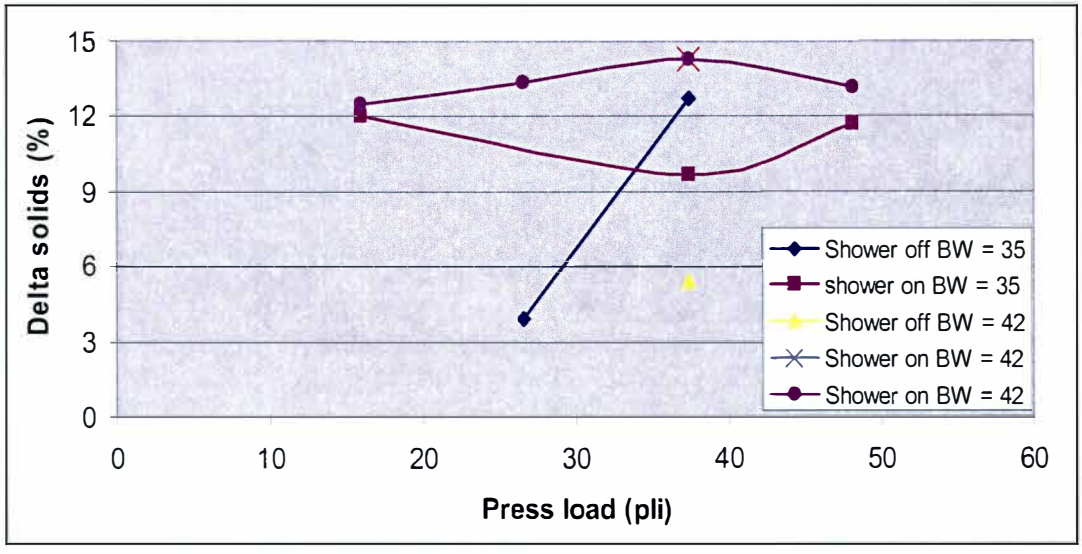

Figure 3.9 Change in solids content vs. press load
(constant m/c speed and different basis weight)

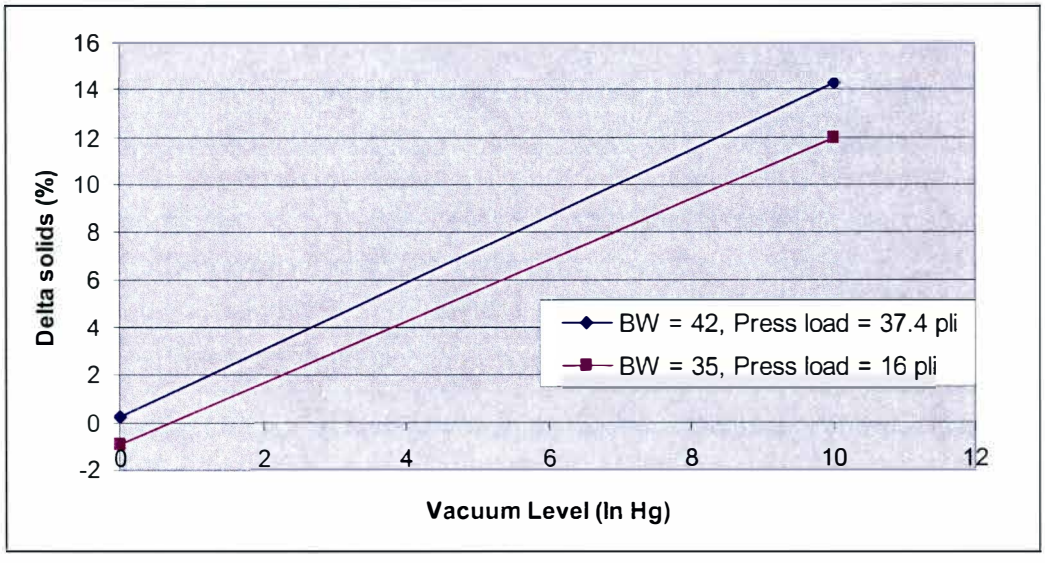

Figure 3.10 Change in solids content vs. vacuum level
(constant press load, m/c speed, and basis weight)

CHAPTER IV

MATHEMATICAL MODELING AND SOLUTION

Introduction

Tests and measurements have been the traditional tools for engineers designing a new product in the paper making industry. Having certain demands for properties of paper and drying requirements, they make changes in input variables to get desired results. This is mainly done by trial and error of experiments. It is a well known fact that even a very small improvement in the paper making process can result in significant savings in cost. For this reason, we need a more accurate knowledge of these processes. One very sophisticated way is to construct a mathematical model and track the paper making by computer simulation tools. These models include some empirical laws and relations which are based on the measurements and the determination of the parameters.

The dewatering in the press section starts when the paper web comes in contact with the RCP roll. Then the paper web progressively dewaters in the different zones of the RCP roll as discussed in Chapter I. Hydraulic pressure differential across the paper web results in dewatering the paper web in consecutive zones of the RCP roll.

To understand the behavior of the RCP roll, a mathematical model for fluid flow across the first layer of mesh covering the RCP roll, is developed. The covering mesh acts as the LOM and offers the maximum resistance to fluid flow across the RCP cylinder. It is assumed that the fluid flow from the second layer of the mesh to the main RCP cylinder is laminar and that these mesh layers do not offer any significant resistance to fluid flow. Additionally, it is assumed that the forces and all other conditions remain

the same along the rotational axis of the RCP roll; there is no change in the dewatering mechanism along the RCP cylinder axis.

The top layer of mesh covering the RCP roll has special characteristics as stated in the RCP technical manual. The pores are evenly distributed in the mesh. The mesh construction is almost similar in warp and shute directions. Pores are circular in cross section[6, 7]. The diameter of the pore is approximately 50μ and the caliper of the mesh layer is about 80μ. The path through the LOM is not straight, but the shape of cross section is almost circular. Due to this characteristic of mesh, the flow is assumed to be similar to the flow in the straight cylindrical capillaries. To simplify the problem, it is assumed that a cylindrical shape capillary represents each hole in the mesh and capillaries are straight. Thus flow through hole will be helpful to understand the behavior of the capillary. The cumulative effect of the flow through the capillaries can predict the behavior of the RCP roll.

Problem statement

At the end of the forming section, formed paper web contains porous area filled with fluid. Figure 4.1 shows sketch of the actual conditions that prevail when the paper web comes in contact with the capillaries of the RCP roll, after the couch roll. Figure 4.1 shows only top three layers of LOM the RCP roll. In the dewatering process, fluid flows from the paper web into the RCP roll through the LOM.

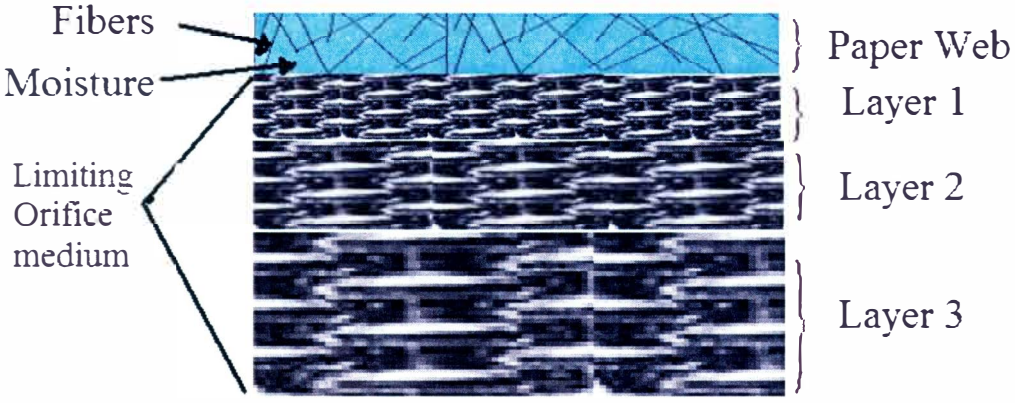

Figure 4.1 Actual condition during dewatering at RCP roll

Because dewatering takes place from the top portion of the RCP roll, it can be said that the fluid flows from the top of the capillary. The paper web first comes in contact with the top layer of the mesh of the LOM. Figure 4.1 shows the fluid locked in porous areas between the fibers in the paper web. Initially, at time $t = 0$, it is assumed that the capillaries in the LOM will be empty and the paper web contains all fluids. The behavior of the fluid flow through the capillaries depends on the forces acting on the fluid in the capillaries and paper web. The behavior of the dewatering can be uniform across the RCP cylinder axis and pores are uniformly distributed over the RCP roll. It is assumed that there is no fiber and air flow in the initial stage of dewatering through LOM. The flow through the capillary is treated as single phase fluid flow and assumed that there is no fiber or air flow through capillaries.

The fluid flow behavior through one capillary will be equivalent to all capillary in the limiting orifice media. The cumulative effect of the dewatering through one capillary will represent overall effect of dewatering behavior or the paper web.

The following section discusses literature reviewed before making the mathematical model of the single phase fluid flow through capillary. The section

following the literature review will show derivation of the mathematical model for flow through a capillary under given force and flow constraints.

Literature review for mathematical model

Research on capillary-driven flow was originally studied more than one century ago. However, it is still a subject of interest due to widespread applications in mechanical industries[12]. For a fully developed capillary driven flow, the analysis on the balance of viscous, surface tension, and gravitational forces yields the classical Washburn equation for the penetration depth, h, and with evolution time, t[13]. While this analysis holds for describing the long-time capillary flow behavior, it does not account for several forces that prevail in the initial stages of a capillary flow process.

Several modifications to the Washburn equation have been reported to include the inertial force and entrance pressure loss effects[14, 15, 16, 17]. Duarte et al.[16] employed a hydrodynamic approach by averaging the Navier-Stokes equation along the liquid column of the capillary geometry. He also considered velocity variation at the entrance. In this approach, the details of liquid motion in the vicinity of flow front are neglected; and the obtained equation is not applicable to the initial time t=0.

Most studies on capillary flow have assumed a constant contact angle between the advancing fluid flow front and the capillary wall. However, experimental observations shown strong dependence of contact angle on the velocity front, time and fluid properties[18, 19, 20]. The Newman model[21] may be applied to all types of capillary flows; however, a fitting parameter in the model must be determined from experimental data. Based on the different considerations of forces, entrance effect, and dynamic contact angle, a set of nonlinear first or second order differential equations were derived in the

literature[13, 15, 16, 17]. The majority of the governing equations were solved using numerical methods. Additionally, analytical solutions were obtained only for several specific cases of capillary flow[12, 21].

None of the literature reviewed above accounts for the influence of centrifugal force over the control volume in the capillary. The capillary orientation is also assumed to be constant throughout the flow process. The fluid flow is always assumed to be either in a horizontal direction or in a vertical upward direction. When fluid flows in upward direction, it is generally known as a capillary rising problem. Many forces have been considered which act on the control volume during dewatering which were not discussed in references reviewed above.

The objective of this section is to develop a mathematical model for capillary flow with conditions that prevail during dewatering the paper web in the press section. The mathematical model is derived similarly as derived in literature reviewed in reference 12. The mathematical model is developed using conservation of mass and linear momentum, subject to the assumptions that the liquid is incompressible, homogeneous, and newtonian.

The final form of capillary rise problem is a second order differential equation as follows and coefficients are obtained depends on prevailing conditions during the capillary filling. The following differential equation shows the capillary rise problem given in reference 12.

$$\left(h + c_1\right)\cdot\frac{d^2h}{dt^2} + c_2\left(\frac{dh}{dt}\right)^2 + \left(c_3\cdot h + c_4\right)\cdot\frac{dh}{dt} + c_5\cdot h + c_6 = 0$$

$$c_1 = h + 1.11\sqrt{BW}$$

$$c_2 = 0.958$$

$$c_3 = \frac{3\mu}{\rho B^2}$$

$$c_4 = \frac{1.772\mu}{\rho\sqrt{BW}}$$

$$c_5 = g$$

$$c_6 = -\frac{\sigma}{\rho}\left(\frac{\cos\theta_d}{B} - \frac{1}{W}\right) \tag{4.1}$$

Where c_1, c_2, c_3, c_4, c_5, c_6 are coefficients of the equation. Coefficients vary according to the prevailing conditions. Reference 15 and 17 showed the analytical solution of the above differential equation and the results were compared with previously obtained experimental results. The results obtained shows good match for given operating conditions and assumptions as shown in Figure 4.2 and 4.3. This section will show the comparison of solution obtained with the MathCAD code and experimental results from references 12 and 14. The MathCAD code for the solution of differential equation is written in the Appendix-I.

Table 4.1 Fluid properties and geometric parameters used in the references 12 and 14.

Fluid	**Geometry**	**Dimensions** mm	**Density** kg/m^3	**Viscosity** Pa*S	**Surface tension** N/m	**Equilibrium Contact Angle** (ϕ_d) deg
Hexane	Parallel Plates	2B = 0.15 2W=25	660.3	0.000326	0.0191	32.7

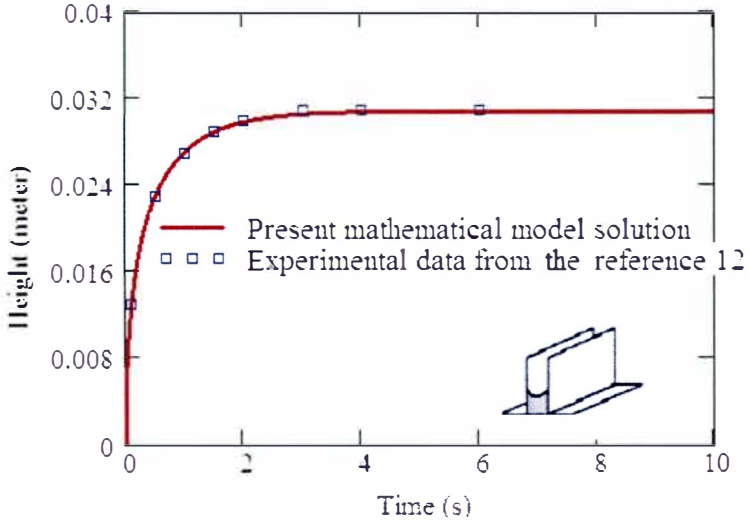

Figure 4.2 Penetration depth vs. time for the capillary flows between two vertical parallel plates.

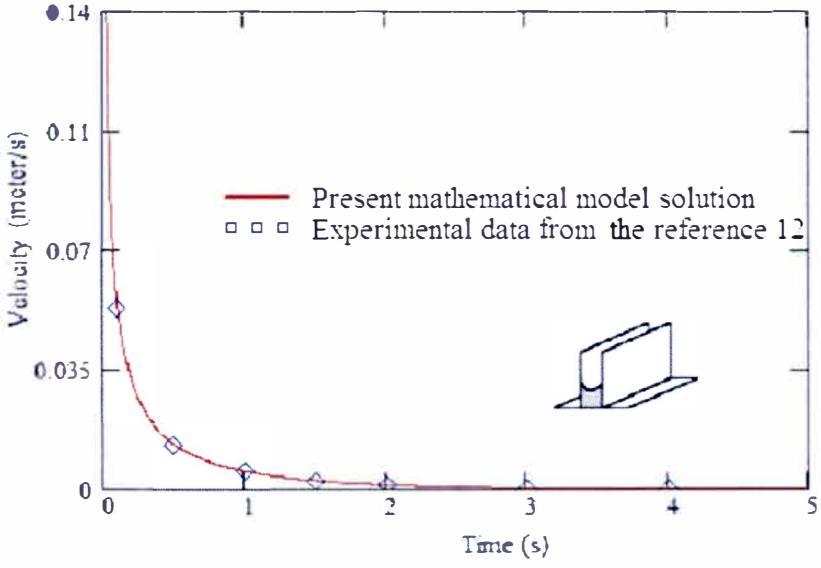

Figure 4.3 Velocity of moving front vs. time for the capillary flows between two vertical parallel plates

The fluid is passing through a cylindrical capillary when the dewatering takes place. We have considered the cylindrical coordinate system, (r, θ, z), to understand the dewatering behavior. The coordinate directions are assumed as shown in Figure 4.4. The origin of the capillary is located at the intersection of vertical z axis and top surface of capillary as shown in the Figure 4.4. The downward direction is considered to be in the

positive-z direction and the upward direction is understood as the negative z direction. Furthermore, the anti-clockwise direction is considered to be the positive θ direction.

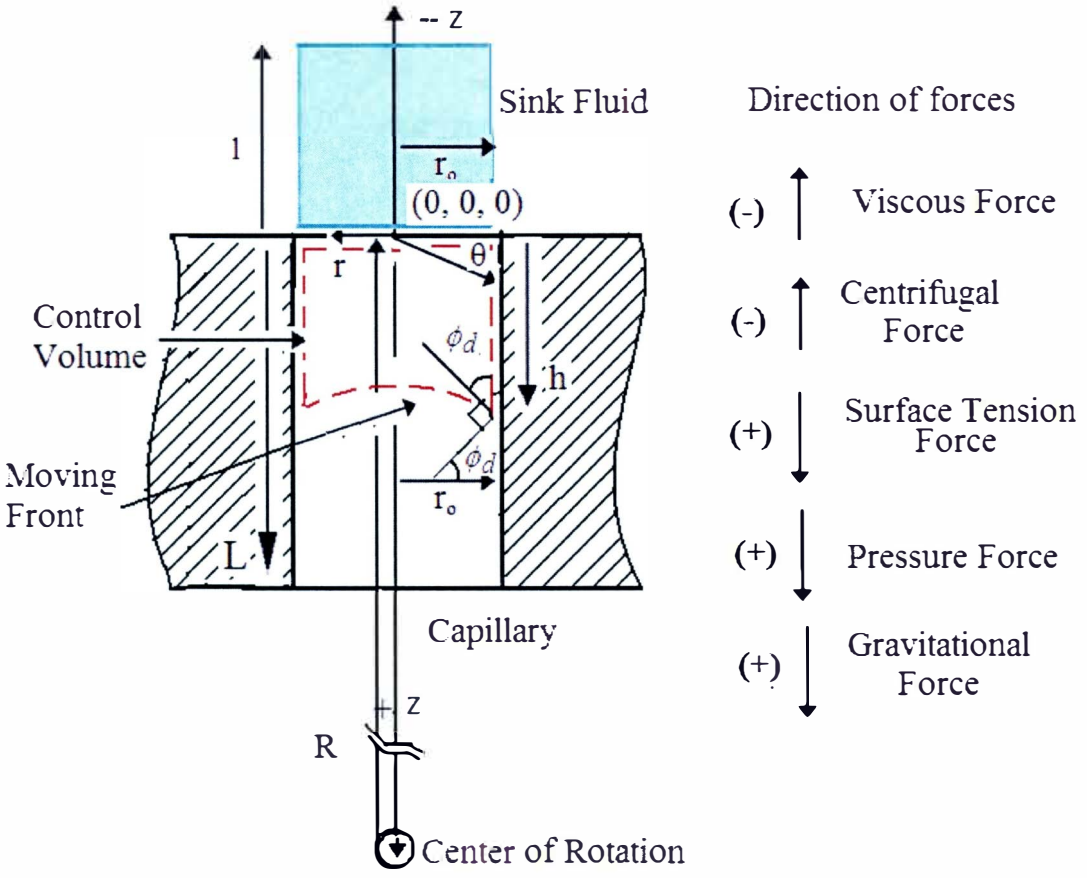

Figure 4.4 Schematic of capillary geometry

The control volume is employed to derive the equation for the dynamics of fluid flow[12, 14]. The fluid in capillary is taken as control volume. We have defined the control volume as shown by the dashed lines in Figure 4.4. The sink fluid shown indicates the fluid in paper web. The travel length along the z direction is referred as the penetration depth h, which is measured from the origin to the valley (or lower peak) point of the surface front. ϕ_d is the angle between capillary wall and tangent to surface front.

Assumptions

The mathematical model development is based on the principle of Conservation of Mass and Momentum, subjected to assumptions as follows,

1. Fluid is incompressible, homogenous, and newtonian.
2. Irrotational fluid flow, $v_\theta = 0$.
3. No flow in radial direction, $v_r = 0$.
4. No change in v_z with respect to θ in capillary tube.
5. Forces acting in downward direction are taken as positive and forces acting upwards are taken as negative.
6. The viscous force brought about by the motion of air in the lower part of the capillary is neglected, since it depends on the density of air which is very small.
7. Flow is assumed to be laminar in nature, i.e. $Re_{max} < 2000$.
8. The parabolic velocity distribution for fully developed flow is taken to approximate the flow, that is, the deviation from the parabolic velocity distribution in the entrance region and at the flow front are ignored.
9. Radius of rotation to calculate the centrifugal force is constant.

Magnitudes of forces are calculated to find important factors governing dewatering of paper web. The values to calculate the forces are taken as follows,

$\rho = 1000 \cdot \frac{kg}{m^3}$ $r_0 = 25 \cdot 10^{-6} \cdot m$ $\Delta p = 2.37 \cdot 10^4 \cdot \frac{N}{m^2}$

$g = 9.807 \frac{m}{s^2}$ $l = 400 \cdot 10^{-6} \cdot m$ $\sigma = 0.072 \cdot \frac{N}{m}$

$\mu = 0.001 \cdot \frac{N \cdot s}{m^2}$ $R = 0.41m$ $h = 100 \cdot 10^{-6} \cdot m$

$\omega = 1.79 \cdot \frac{rad}{s}$ $v = 0.1 \cdot \frac{m}{s}$ $\phi_d = 0$

The forces acting on the control volume in capillary approximately calculated as follows:

$$\text{Gravitational Force} = \rho \cdot g \cdot \pi \cdot r_0^2 \cdot (h + l) = 9.628 \times 10^{-9} \cdot N$$

$$\text{Centrifugal Force} = \rho \cdot \omega^2 \cdot \pi \cdot r_0^2 \cdot (h + l) \cdot (l + R) = 8.999 \times 10^{-10} \, N$$

$$\text{Pressure Force} = \Delta p \cdot \pi \cdot r_0^2 = 4.653 \times 10^{-5} \, N$$

$$\text{Viscous Force} = 8 \cdot h \cdot \pi \cdot \mu \cdot v = 1.005 \times 10^{-6} \, N$$

$$\text{Surface Tension} = 2 \cdot \pi \cdot r_0 \cdot \sigma \cos(\phi_d) = 1.162 \times 10^{-5} \, N$$

$$Netforce := \text{Gravitational Force} - \text{Centrifugal Force} + \text{Pressure Force} - \text{Viscous Force} + \text{Surface Tension}$$

$$Netforce = 1.65 \times 10^{-4} \cdot N$$

The calculation above shows the magnitude of the forces. The pressure force is the dominating forces in the direction of flow. The viscous force is the dominating force acting in the opposite direction of the flow. The gravitational force and the centrifugal force are not the major forces that govern the fluid flow through the capillary.

To find the surface tension force, the accurate geometry of the surface front and capillary media are required. The maximum surface tension force for $\phi_d = 0$ is much smaller than the pressure force and thus surface tension force is neglected in the model derivation.

Considering the deformable control volume encompassing the penetrated region in the capillary as shown in Figure 4.4, the integral momentum equation in z-direction may be written as[12, 14, 20],

$$\Sigma F_z = \frac{d}{dt}\left(\int_0^h \int_0^{r_0} \int_0^{2\cdot\pi} \rho \cdot v_z \, d\theta \cdot r \, dr \, dz \right) + \int_0^{2\cdot\pi} \int_0^{r_0} v_z \cdot (\rho \cdot v_z) \cdot r \, dr \, d\theta \tag{4.2}$$

Where, ΣF_z denotes the sum of forces acting on the control volume in z direction. To evaluate the right side of the equation (4.2), the information on the velocity profile of fluid in the capillary is required. Since it is assumed that the flow in capillary is laminar in nature, a fully developed flow with parabolic profile for velocity v_z can be obtained from Poiseuille's flow equation[17]. As we have neglected surface tension force for capillary flow, it can be assumed that the velocity of surface front follows Poiseuille's flow equation and moves at the same speed as of fully developed fluid flow.

$$v_z = 2 \cdot \frac{dh}{dt}\left[1 - \left(\frac{r}{r_0} \right)^2 \right] \tag{4.3}$$

Now solving first term on right side of integral momentum equation (4.2),

$$M_b = \frac{d}{dt}\left(\int_0^h \int_0^{r_0} \int_0^{2\cdot\pi} \rho \cdot v_z \, d\theta \cdot r \, dr \, dz \right) \tag{4.4}$$

Substituting v_z from equation (4.3) in equation (4.4),

$$M_b = \frac{d}{dt}\left[\int_0^h \int_0^{r_0} \int_0^{2\cdot\pi} \rho\cdot 2\cdot\frac{dh}{dt}\left[1-\left(\frac{r}{r_0}\right)^2\right] d\theta\cdot r\, dr\, dz\right]$$

$$M_b = \frac{d}{dt}\left[\int_0^h \int_0^{r_0} 4\cdot\pi\rho\cdot\frac{dh}{dt}\left[1-\left(\frac{r}{r_0}\right)^2\right]\cdot r\, dr\, dz\right]$$

Integrating and substituting the limits with respect to r in equation above,

$$M_b = \frac{d}{dt}\left[\int_0^h \pi\cdot(r_0)^2\cdot\rho\cdot\frac{dh}{dt}\, dz\right]$$

$$M_b = \frac{d}{dt}\left[h\cdot\pi\cdot(r_0)^2\cdot\rho\cdot\frac{dh}{dt}\right]$$

$$M_b = \left[\pi\cdot\rho\cdot h\cdot(r_0)^2\cdot\frac{d^2h}{dt^2}\right] + \pi\cdot\rho\cdot(r_0)^2\cdot\left(\frac{dh}{dt}\right)^2 \qquad (4.5)$$

Now, solving second term on the right side of the integral momentum equation (4.2),

$$M_s = \int_0^{2\pi} \int_0^{r_0} v_z\cdot(\rho\cdot v_z)\cdot r\, dr\, d\theta \qquad (4.6)$$

Substituting v_z from equation (4.3) into equation (4.6),

$$M_s = \int_0^{2\pi} \int_0^{r_0} 2\cdot\frac{dh}{dt}\cdot\left[1-\left(\frac{r}{r_0}\right)^2\right]\cdot\rho\cdot 2\cdot\frac{dh}{dt}\cdot\left[1-\left(\frac{r}{r_0}\right)^2\right]\cdot r\, dr\, d\theta$$

$$M_s = \int_0^{2\pi} \int_0^{r_0} 4\cdot\left(\frac{dh}{dt}\right)^2\cdot r\cdot\left[1-\left(\frac{r}{r_0}\right)^2\right]^2\cdot\rho\, dr\, d\theta$$

Integrating and substituting the limits with respect to r in equation above,

$$M_S = \frac{4}{3}\cdot\pi\cdot(r_0)^2\cdot\rho\cdot\left(\frac{dh}{dt}\right)^2 \tag{4.7}$$

To solve the left side of the equation (4.2) we need to know the forces acting on the control volume. There are two types of forces acting on the control volume namely, body forces F_b and surface forces F_s.

$$\Sigma F_z = F_b + F_s \tag{4.8}$$

Body forces include gravitational force F_{bg} and centrifugal force F_{bc} of control volume. The centrifugal force acting on the control volume depend on the radius of rotation of capillary. In present case change in centre of mass of control volume is negligible compare to radius of rotation and thus change in radius of rotation is negligible. Therefore in our case, radius of rotation is assumed to be constant and taken as a distance between center of mass of control volume and axis of rotation of RCP roll.

All the body forces can be defined as follows,

$$F_b = F_{bg} + F_{bc} \tag{4.9}$$

Gravitational force on the control volume F_{bg},

$$F_{bg} = \int_0^h \int_0^{r_0} \int_0^{2\cdot\pi} \rho\cdot g\, d\theta\cdot r\, dr\, dz$$

$$F_{bg} = \pi\cdot(r_0)^2\cdot h\cdot\rho\cdot g \tag{4.10}$$

Centrifugal force on the control volume F_{bc},

$$F_{bc} = -\int_0^h \int_0^{r_0} \int_0^{2\cdot\pi} \rho\cdot\omega^2\cdot R\, d\theta\cdot r\, dr\, dz$$

$$F_{bc} = -\pi\cdot(r_0)^2\cdot h\cdot\rho\cdot\omega^2\cdot R \tag{4.11}$$

Substituting (4.10) and (4.11) in equation (4.9)

$$F_b = \left[\pi \cdot (r_o)^2 \cdot h \cdot \rho \cdot g\right] - \pi \cdot (r_o)^2 \cdot h \cdot \rho \cdot \omega^2 \cdot R \tag{4.12}$$

The surface forces include forces acting on cylindrical surface F_{sc} and forces acting on surface front F_{sf}. Forces acting on the surface front are governed by *Young-Laplace equation*[22], which is derived from centrifugal force due to sink fluid F_{sfc}, pressure force on the surface front F_{sfp} due to pressure differential between ambient pressure and internal pressure in the RCP roll, and gravitational force of sink fluid F_{sfg}. Surface force act along the cylindrical surface F_{sc} is viscous force of flowing fluid.

All the surface forces can be defined as follows,

$$F_s = F_{sc} + F_{sf} \tag{4.13}$$

Surface forces act on the cylindrical surface F_{sc},

$$F_{SC} = \int_0^h \int_0^{2\pi \cdot r_0} \tau_w \, d\theta \, dz \tag{4.14}$$

where τ_w can be obtained by[12],

$$\tau_w = \mu \cdot \frac{dv_r}{dr}$$

$$\tau_w = \mu \cdot \frac{d}{dr}\left[2 \cdot \frac{dh}{dt} \cdot \left[1 - \left(\frac{r}{r_0} \right)^2 \right] \right]_{\text{at } r = r_0}$$

$$\tau_w = -4 \cdot \frac{\mu}{r_0} \cdot \frac{dh}{dt} \tag{4.15}$$

Substituting τ_w in F_{sc} (4.14),

$$F_{SC} = -8 \cdot h \cdot \pi \cdot \mu \cdot \frac{dh}{dt} \tag{4.16}$$

Forces acting on surface front F_{sf},

$$F_{sf} = F_{sfc} + F_{sfg} + F_{sfp} \tag{4.17}$$

where F_{sfc}, F_{sfg}, F_{sfp} can be defined as follows.

Centrifugal force on the sink fluid F_{sfc},

$$F_{sfc} = -\int_0^l \int_0^{r_0} \int_0^{2\cdot\pi} \rho\cdot\omega^2\cdot R\, d\theta\cdot r\, dr\, dz$$

$$F_{sfc} = -\pi\cdot(r_0)^2\cdot l\cdot\rho\cdot\omega^2\cdot R \tag{4.18}$$

Gravitational force of the sink fluid F_{sfg},

$$F_{sfg} = \int_0^l \int_0^{r_0} \int_0^{2\cdot\pi} \rho\cdot g\, d\theta\cdot r\, dr\, dz$$

$$F_{sfg} = \pi\cdot(r_0)^2\cdot l\cdot\rho\cdot g \tag{4.19}$$

Atmospheric pressure differential force on moving front F_{sfp},

$$F_{sfp} = \pi\cdot(r_0)^2\left[(p_0 - p_i) - 1.11\cdot\rho\cdot\sqrt{\pi\cdot r_0^2}\cdot\frac{d^2h}{dt^2}\right] \tag{4.20}$$

Substituting F_{sfc} (4.18), F_{sfg} (4.19), and F_{sfp} (4.20) in equation F_{sf} (4.16)

$$F_{sf} = -\pi\cdot(r_0)^2\cdot l\cdot\rho\cdot\omega^2\cdot R + \pi\cdot(r_0)^2\cdot l\cdot\rho\cdot g + \pi\cdot(r_0)^2\cdot(p_0 - p_i)$$

$$F_{sf} = \pi\cdot(r_0)^2\cdot\rho\left[-l\cdot\omega^2\cdot R + l\cdot g + \left(\frac{p_0 - p_i}{\rho}\right) - 1.11\cdot\sqrt{\pi\cdot r_0^2}\cdot\frac{d^2h}{dt^2}\right] \tag{4.21}$$

Now finding net surface forces by substituting (4.16) and (4.21) in (4.13).

$$F_s = \pi\cdot(r_0)^2\cdot\rho\left[-l\cdot\omega^2\cdot R + l\cdot g + \left(\frac{p_0 - p_i}{\rho}\right) - 1.11\cdot\sqrt{\pi\cdot r_0^2}\cdot\frac{d^2h}{dt^2}\right] - 8\cdot h\cdot\pi\cdot\mu\cdot\frac{dh}{dt} \tag{4.22}$$

Thus ΣF_z can be given by substituting (4.22) and (4.12) in (4.8),

$$\Sigma F_z = \pi\cdot(r_0)^2\cdot\rho\cdot\left[-l\cdot\omega^2\cdot R + l\cdot g + \left(\frac{p_0 - p_i}{\rho}\right) - 1.11\cdot\sqrt{\pi\cdot r_0^2}\cdot\frac{d^2h}{dt^2}\right]$$

$$-8\cdot h\cdot\pi\cdot\mu\cdot\frac{dh}{dt} + \left[\pi\cdot(r_0)^2\cdot h\cdot\rho\cdot g - \pi\cdot(r_0)^2\cdot h\cdot\rho\cdot\omega^2\cdot R\right] \tag{4.23}$$

Now substituting ΣF (4.23), M_b (4.5) and M_s (4.7) in (4.23) and then simplifying,

$$\pi\cdot(r_0)^2\cdot\rho\cdot\left[-l\cdot\omega^2\cdot R + l\cdot g + \left(\frac{p_0 - p_i}{\rho}\right) - 1.11\cdot\sqrt{\pi\cdot r_0^2}\cdot\frac{d^2h}{dt^2}\right]$$

$$-8\cdot h\cdot\pi\cdot\mu\cdot\frac{dh}{dt} + \left[\pi\cdot(r_0)^2\cdot h\cdot\rho\cdot g - \pi\cdot(r_0)^2\cdot h\cdot\rho\cdot\omega^2\cdot R\right]$$

$$= \left[\pi\cdot\rho\cdot h\cdot(r_0)^2\cdot\frac{d^2h}{dt^2}\right] + \pi\cdot\rho\cdot(r_0)^2\cdot\left(\frac{dh}{dt}\right)^2 + \frac{4}{3}\cdot\pi\cdot(r_0)^2\cdot\rho\cdot\left(\frac{dh}{dt}\right)^2$$

$$\left(h + 1.11\cdot\sqrt{\pi\cdot r_0^2}\right)\cdot\frac{d^2h}{dt^2} + \left(\frac{7}{3}\right)\cdot\left(\frac{dh}{dt}\right)^2 + \frac{8\cdot h\cdot\mu}{(r_0)^2\cdot\rho}\cdot\frac{dh}{dt} + \left(-g + \omega^2\cdot R\right)\cdot h$$

$$+\left(l\cdot\omega^2\cdot R - l\cdot g - \frac{p_0 - p_i}{\rho}\right) = 0 \tag{4.24}$$

Equation (4.24) can be simply written as,

$$\left(h + c_1\right)\cdot\frac{d^2h}{d\cdot t^2} + c_2\left(\frac{dh}{dt}\right)^2 + \left(c_3\cdot h + c_4\right)\cdot\frac{dh}{dt} + c_5\cdot h + c_6 = 0 \tag{4.25}$$

Where c_1, c_2, c_3, c_4, c_5, c_6 are coefficients of the equation and given as follows,

$$c_1 = 1.11 \cdot \sqrt{\pi \cdot r_0^2}$$

$$c_2 = \frac{7}{3}$$

$$c_3 = \frac{8 \cdot \mu}{(r_0)^2 \cdot \rho}$$

$$c_4 = 0$$

$$c_5 = \left(-g + \omega^2 \cdot R\right)$$

$$c_6 = \left(l \cdot \omega^2 \cdot R - l \cdot g - \frac{p_0 - p_i}{\rho}\right)$$

Equation (4.25) is solved to understand the behavior of the RCP roll using MathCAD code shown in Appendix A. Figure 4.5 and Figure 4.6 shows behavior of capillary height and velocity of fluid front in capillary tube with respect the time.

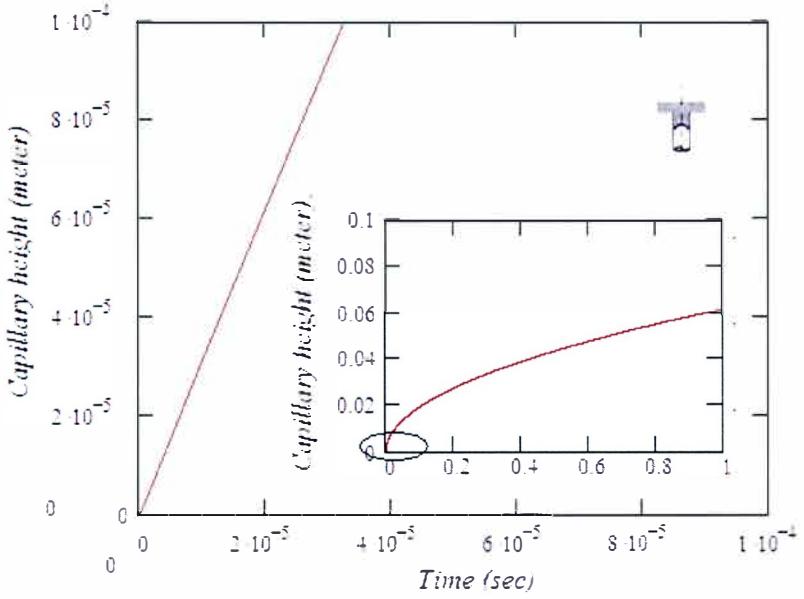

Figure 4.5 Height of surface front vs. time

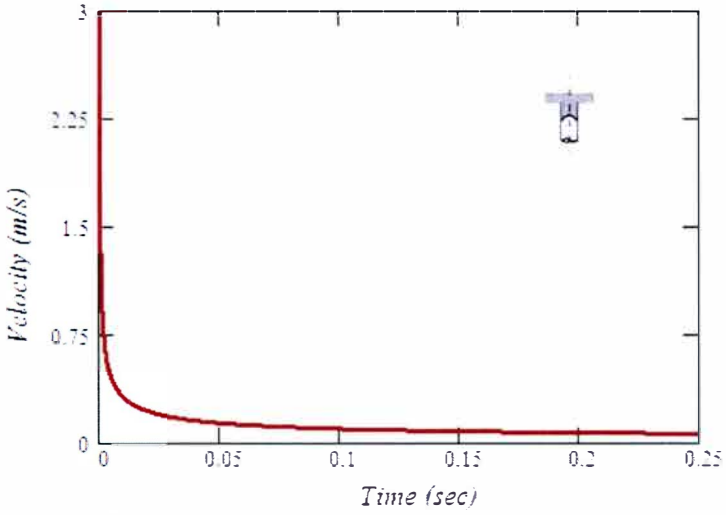

Figure 4.6 Velocity of surface front vs. time

Figure 4.5 and Figure 4.6 shows decrease in velocity of flowing front and increase in height of surface front in capillary. The height is keep increasing because the forces are not balanced and acceleration is decreasing with increase in time. Figure 4.5 shows time required to fill the capillary height up to LOM. In RCD process the thickness of top layer of LOM is 100μ. Figure 4.5 shows time required to reach 100μ is approximately 30μs.

CHAPTER V

CONCLUSIONS

Several important observations were made from the experiments performed. These observations were organized into two sections. First section focused on the machine variables of the RCD technology. Second section focused on the pulp characteristics affecting the RCD technology behavior.

Machine variables

Effects of press load, vacuum level, and cleaning shower conditions are studied as machine variables. The dewatering behavior of the RCP roll matched the expected theory. The experiments at paper pilot plant at WMU facility shown that press load, vacuum level and shower condition have significant impact on water removal rate.

The vacuum below breakthrough level does not result into significant dewatering but vacuum level equal or above breakthrough results in significant dewatering. With proper vacuum level, up to 1 - 5 lb/lb of moisture removal can be obtained. We have obtained approximately 2lb/lb of moisture removal for 14 inHg, approximately 5 lb/lb moisture removal for 10 inHg, and approximately 2lb/lb of moisture removal for 5 inHg of vacuum level in the RCP roll. Results shows very high vacuum is also results in poor dewatering of paper web.

Press load has varying effect on the dewatering behavior. Result shows increase up to 0.75 lb/lb dewatering capacity with increase of press load up to 30pli. Results shows after certain increase in press load the dewatering behavior remains constant.

Press load is also important from paper properties point of view and supports following conclusions but database is limited. Press load has ordinary effect on the caliper of paper sheet. Result shows 5% increase in paper caliper for 300% increase in the press load. Press load has significant effect on the porosity of paper sheet. Results shows 50% decrease in porosity for 300% increase in the press load. Press load has ordinary effect on strength properties of paper sheet. Result shows approximately 15% increase in tensile strength and approximately 7% of increase in tear strength for 300% increase in press load.

Machine speed also governs the dewatering efficiency of machine. Result shows linear decrease in change of moisture content for paper web with increase in machine speed. However water removal rate is higher at higher machine speeds. Result shows increase of approximately 1 lb/lb water removal for increase from 50 fpm to 70 fpm in machine speed.

The internal cleaning shower also plays critical role in dewatering process. The internal shower helps to clean interior of the RCP roll and remove any blockage caused by the paper web fibers and improves the dewatering efficiency. The dewatering efficiency increases by 75% for turning on the internal shower.

Pulp and paper properties

Effects of fiber furnishes, on the dewatering behavior is studied as machine variables. Higher hardwood fiber content in pulp results in better dewatering behavior of the wet paper web. Results shows approximately 2 lb/lb of moisture removal for 90% southern softwood and 10% southern hardwood fiber furnish and approximately 5 lb/lb of moisture removal rate for 40% southern softwood with 60% southern hardwood fiber

furnish at given freeness and other machine operating conditions. The RCD technology has improved performance for pulp having higher hardwood fiber furnish.

Individual forces

Individual forces are derived and resulting forces are calculated. Pressure force is mainly dominating force in direction of flow. Viscous is dominating force acting in opposite direction of the flow. Gravitational force and centrifugal force are not major forces that govern the fluid flow through the capillary.

Mathematical model

Mathematical model is derived by considering a deformable control volume encompassing the penetrated region in the capillary. In derivation of mathematical model minor forces due to capillary action due to paper web fibers and surface tension due to air are ignored. Mathematical model is solved using the MathCAD code. Results obtained from numerical solution show good match with previously performed experiments. The solution shows increase in height of surface front in capillary and decrease in velocity with respect to time. By using the MathCAD code developed, result shows that for the present RCD operation condition, approximately 30μs is needed to fill capillary of 100μm.

Further development work

The RPD technology has adequately demonstrated its technical effectiveness at speeds up to 70 fpm. Further development work would involve the following,

- Further pilot scale trials to confirm consistent runnability at high speeds.

- Further pilot scale trials to refine the operating levels for maximum water removal for various grades of tissue/toweling.
- Mathematical model development using more precise approaches and careful consideration of machine variable, pulp properties, and paper properties to predict the behavior of RCD technology.

APPENDIX A

MATHCAD CODE

Following is general second order differential equation for the capillary rise problem. '*rkfixed*' uses the fourth order Runge-Kutta method to solve a first order differential equation. To make use of *'rkfixed'* method to solve second order differential equation, equation is first transformed in to two first order differential equations as Runga-Kutta method can not solve second order differential equation. Equation (4.1) is divided in two first order equation as shown below. Two differential equations are solved using matrix and function '*rkfixed*'.

$$(h + c_1)\frac{d^2h}{dt^2} + c_2\left(\frac{dh}{dt}\right)^2 + (c_3h + c_4)\frac{dh}{dt} + c_5h + c_6 = 0 \qquad (4.1)$$

$$(X + c_1)\cdot X'' + c_2\cdot X'^2 + (c_3\cdot X + c_4)\cdot X' + c_5\cdot X + c_6 = 0$$

$X' =$ () First Differential Equation

$$X'' = \frac{-1}{(X_0 + c_1)}\cdot\left[c_2\cdot X_1'^2 + (c_3\cdot X_0 + c_4)\cdot X_1 + c_5\cdot X_0 + c_6\right]$$ Second Differential Equation

x := 0 v := 0 $X := \begin{pmatrix} x \\ v \end{pmatrix}$ Initial conditions

tstart := 0 tend := t Time range from 0 to t seconds

$$DX(t, X) := \begin{bmatrix} X_1 \\ \frac{-1}{(X_0 + c_1)}\cdot\left[c_2\cdot X_1'^2 + (c_3\cdot X_0 + c_4)\cdot X_1 + c_5\cdot X_0 + c_6\right] \end{bmatrix}$$ First Differential Equation; Second Differential Equation

$Xstart := \begin{pmatrix} 0 \\ 1 \end{pmatrix}$ npoints := 10000 npoints is number of points between starting and ending of experiment

F := rkfixed(Xstart, tstart, tend, npoints, DX)

BIBLIOGRAPHY

1. Richard A. Reese, "Paper machine wet press manual." Fourth Edition TAPPI press (1999)
2. Joachim Petrini, "Master's Thesis: On the role of evaporation processes during impulse pressing of paper." Luleå University of Technology, Stockholm, Sweden (May, 2001)
3. Smook G. A., "Handbook for pulp & paper technologists." Second Edition, Angus Wilde Publications (1994)
4. Osman Polat, "Special Report Rigid Capillary Pressing (RCP) Development", (Dec 17 2002)
5. Valmet-Karlstad AB, Internal construction of RCP roll, RCP technical manual (August 16, 1999)
6. Stelljes, JR. et al. "Method of drying fibrous structures" The Procter & Gamble Company. United States Patent US 2003/0033727 A1. (Feb. 20, 2003)
7. Ensign et al. "Limiting orifice drying of cellulosic fibrous structures, apparatus therefore, and cellulosic fibrous structures produced thereby" The Procter & Gamble Company, Cincinnati, Ohio. United States patent 5,437,107 (August 1, 1995)
8. Osman Polat, "Rigid Capillary Pressing (RCP) file memo", Procter & Gamble Company (January 2, 2003)
9. Steven W. Burton, "Doctor's Dissertation: An investigation of Z-direction density profile development during impulse drying." The institute of Paper Chemistry Appleton, Wisconsin. (January-1987, Reprint October-1990)

10. Hughes, John, "Masters Thesis: The effects of selected pilot paper machine variables on web shrinkage" Western Michigan University. (1971)

11. Pulp & Paper resources & information site: www.paperonweb.com

12. Yan Xiao, Fuzheng Yang, Pitchumani Ranga, "A generalized analysis of capillary flows in channels" Journal of Colloid and Interface Science. (February 15, 2006)

13. Washburn W. Edward, "The dynamics of capillary flow", The Physical review. 17 (1921) 273.

14. Barraza H. J., Kunapuli S., O'Rear E.A., Journal of Physical Chemistry. B 106 (2006) 4979.

15. Rainskinmaki P., Manesh A. S., Jasberg A., Kaponen A., Merikoski J., Timonen J., Journal of Stat. Physics. 107 (2002) 143.

16. Duarte A. A., Strier D. E., Zanette D. H., American Journal of physics, 64 (1996) 413.

17. Levine S., Reed P., Watson E. J., Kerker M. (Ed.), Colloid and Interface Science, vol. III: Adsorption, Catalysis, Solid Surfaces, Wetting, Surface Tension, and Water, Academic Press, New York, 1976, P. 403.

18. Berzkin V. V., Churaev N. V., Colloid J. USSR 44 (1982) 376.

19. Hamraoui A., Thuresson K., Nylander T., Yaminsky Y., Journal of Colloid Interface Science, 226 (2000)199.

20. Hamraoui A., Nylander T., Journal of Colloid Interface Science 250 (2002) 415.

21. Newman S., Journal of Colloid and Interface science 26.(1968)209

22. Zhmud B. V. Delgado A. Rath H. J., Microgravity Science Technology. 4 (1993) 203.